Electronic Supplementary Material (ESI) for Journal of Materials Chemistry A.

Judicious engineering of a metal-free perylene dye for high-efficiency dye sensitized solar cells: the control of excited state and charge carrier dynamics

Lin Yang,[a] Shu Chen,[bc] Jing Zhang,[a] Junting Wang,[bc] Min Zhang,*[b] Xiandui Dong[b] and Peng Wang*[a]

[a] *Department of Chemistry, Zhejiang University, Hangzhou, 310028, China. E-mail: pw2015@zju.edu.cn*

[b] *Changchun Institute of Applied Chemistry, Chinese Academy of Sciences, Changchun, 130022, China. E-mail: min.zhang@ciac.ac.cn*

[c] *University of Chinese Academy of Sciences, Beijing, 100049, China*

Materials and synthesis

Tris(dibenzylideneacetone)dipalladium ($Pd_2(dba)_3$), tris(1,1-dimethylethyl)phosphine (P(*t*-Bu)$_3$), bis(2',6'-diisopropoxybiphenyl)cyclohexylphosphine (Ruphos), sodium *tert*-butoxide (NaO*t*-Bu), Cs_2CO_3, and KOH were obtained from Sigma-Aldrich. 1,4-Dioxane, toluene, THF, and ethanol were distilled before use. 4-(4,4-Dihexyl-4*H*-cyclopenta[1,2-*b*:5,4-*b*']dithiophen-2-yl)-*N*,*N*-bis(4-(hexyloxy)phenyl)aniline,[S1] butyl 4-(7-ethynylbenzo[*c*][1,2,5]thiadiazol-4-yl)benzoate,[S2] 4-(1-(2-hexyldecyl)-6*b*,10-dihydro-1*H*-phenanthro[1,10,9,8-*cdefg*]carbazol-3-yl)-*N*,*N*-bis(4-(hexyloxy)phenyl)aniline,[S3] bis(2',4'-bis(hexyloxy)-[1,1'-biphenyl]-4-yl)amine,[S4] and 3-bromo-1-(2-hexyldecyl)-1*H*-phenanthro[1,10,9,8-*cdefg*]carbazole[S5] were prepared according to the correspondent literature methods. Other chemicals were purchased and used without further purification. The synthetic details for **SC1**, **SC2**, and **SC3** are described as follows.

*4-(7-((6-(4-(Bis(4-(hexyloxy)phenyl)amino)phenyl)-4,4-dihexyl-4H-cyclopenta[1,2-b:5,4-b']dithiophen-2-yl)ethynyl)benzo[c][1,2,5]thiadiazol-4-yl)benzoic acid (**SC-1**)*: In a three-neck round bottom flask, 4-(4,4-dihexyl-4*H*-cyclopenta[1,2-*b*:5,4-*b*']dithiophen-2-yl)-*N*,*N*-bis(4-(hexyloxy)phenyl)aniline (789 mg, 1.00 mmol) was dissoved with THF (30 mL) before the dropwise addition of NBS (196 mg, 1.10 mmol) in THF (10 mL). The reaction mixture was stirred at RT for 1 h. Water was then added to terminate the reaction and the mixture was extracted three times with chloroform. The organic phase was washed with water and then dried over anhydrous sodium sulfate. After solvent removal under reduced pressure, the residue was purified by column chromatography (toluene/petroleum ether 60–90 °C, *v*/*v*, 1/40) on silica gel to yield a yellow oil as the desired product 4-(6-bromo-4,4-dihexyl-4*H*-cyclopenta[1,2-*b*:5,4-*b*']dithiophen-2-yl)-*N*,*N*-bis(4-(hexyloxy)phenyl)aniline. Then, to a dried Schlenk tube were added 4-(10-bromo-1-(2-hexyldecyl)-1*H*-phenanthro[1,10,9,8-*cdefg*]carbazol-3-yl)-*N*,*N*-bis(4-(hexyloxy)phenyl)aniline, butyl 4-(7-ethynylbenzo[*c*][1,2,5]thiadiazol-4-yl)benzoate (337 mg, 1.00 mmol), $Pd_2(dba)_3$ (34 mg, 0.04 mmol), P(*t*-Bu)$_3$ (0.09 mL, 0.04 mmol, 10 wt% in toluene), Cs_2CO_3 (218 mg, 0.66 mmol), and dioxane (10 mL) in a nitrogen-filled glovebox. The reaction mixture was refluxed under argon for 5 h. Water was added and the mixture was extracted three times with chloroform. The organic phase was washed with water and then dried over anhydrous sodium sulfate. After solvent removal under reduced pressure, the residue was purified by column chromatography (toluene/petroleum ether 60–90 °C, *v*/*v*, 1/1) on silica gel to yield a red solid as the desired butyl ester. Then in a three-neck round bottom flask, the butyl ester and KOH (146 mg, 2.60 mmol) were dissoved in THF/H_2O (10 mL, *v*/*v*, 3/1). The mixture was refluxed for 8 h. Water and chloroform were then added. The organic phase was washed with 0.2 M phosphoric acid aqueous solution and water in turn, and then dried over anhydrous sodium sulfate. After removing the solvent under reduced pressure, the crude product was purified by column chromatography (chloroform/methanol, *v*/*v*, 20/1) on silica gel to yield a black solid as the final product **SC-1** (768 mg, 72% yield). Melting point: 187–189 °C. ^{1}H NMR (400 MHz, THF-d_8) δ: 8.17 (br, 4H), 7.95–7.93 (m, 1H), 7.89 (d, J = 7.5 Hz, 1H), 7.49–7.40 (m, 3H), 7.26 (s, 1H), 7.09–7.01 (m, 4H), 6.90–6.88 (m, 3H), 6.85–6.83 (m, 3H), 3.95–3.92 (m, 4H), 2.07–2.02 (m, 4H), 1.37–1.36 (m, 8H), 1.29 (br, 12H), 1.19 (br, 12H), 0.92–0.89 (m, 6H), 0.84–0.80 (m, 6H). ^{13}C NMR (100 MHz, THF-d_8) δ: 167.52, 162.20, 157.08, 156.14, 154.16, 149.64, 148.18, 142.10, 141.55, 141.18, 136.05, 135.96, 134.82, 133.78, 132.57, 131.84, 130.76, 130.36, 130.11, 129.37, 128.17, 127.60, 126.84, 126.11, 121.49, 119.95, 117.31, 116.29, 116.20, 92.57, 68.94, 57.34, 55.21, 39.04, 32.76, 30.86, 30.80, 30.65, 30.50, 37.50, 26.91, 23.70, 14.54. HR-MS (MALDI-TOF) *m*/*z* calcd. for ($C_{66}H_{73}N_3O_4S_3$): 1067.47632. Found: 1067.47589. Anal. Calcd. for $C_{66}H_{73}N_3O_4S_3$: C, 74.19; H, 6.89; N, 3.93. Found: C, 74.17; H, 6.92; N, 3.91%.

*4-(7-((10-(4-(Bis(4-(hexyloxy)phenyl)amino)phenyl)-1-(2-hexyldecyl)-1H-phenanthro[1,10,9,8-cdefg]carbazol-3-yl)ethynyl)benzo[c][1,2,5]thiadiazol-4-yl)benzoic acid (**SC-2**)*: In a three-neck round bottom flask, 4-(1-(2-hexyldecyl)-6*b*,10-dihydro-1*H*-phenanthro[1,10,9,8-*cdefg*]carbazol-3-yl)-*N*,*N*-bis(4-(hexyloxy)phenyl)aniline (1.13 g, 1.21 mmol) was dissoved with THF (30 mL). The solution was cooled to 0 °C by use of an ice salt bath before the dropwise addition of NBS (216 mg, 1.21 mmol) in THF (10 mL). The reaction mixture was stirred at 0 °C for 0.5 h. Water was then added to terminate the reaction and the mixture was extracted three times with chloroform. The organic phase was washed with water and then dried over anhydrous sodium sulfate. After solvent removal under reduced pressure, the residue was purified by column chromatography (toluene/petroleum ether 60–90 °C, *v*/*v*, 1/50) on silica gel to yield a yellow oil as the desired product 4-(10-bromo-1-(2-hexyldecyl)-1*H*-phenanthro[1,10,9,8-*cdefg*]carbazol-3-yl)-*N*,*N*-bis(4-(hexyloxy)phenyl)aniline. Then, to a dried Schlenk tube were added 4-(10-bromo-1-(2-hexyldecyl)-1*H*-phenanthro[1,10,9,8-*cdefg*]carbazol-3-yl)-*N*,*N*-bis(4-(hexyloxy)phenyl)aniline, butyl 4-(7-ethynylbenzo[*c*][1,2,5]thiadiazol-4-yl)benzoate (199 mg, 0.59 mmol), $Pd_2(dba)_3$ (17 mg, 0.02 mmol), P(*t*-Bu)$_3$ (0.045 mL, 0.02 mmol, 10 wt% in toluene), Cs_2CO_3 (108 mg, 0.33 mmol), and dioxane (10 mL) in a nitrogen-filled glovebox. The reaction mixture was refluxed under argon for 5 h. Water was added and the mixture was extracted three times with chloroform. The organic phase was washed with water and then dried over anhydrous sodium sulfate. After solvent removal under reduced pressure, the residue was purified by column chromatography (toluene/petroleum ether 60–90 °C, *v*/*v*, 1/1) on silica gel to yield a red solid as the desired butyl ester. Then in a three-neck round bottom flask, the butyl ester and KOH (146 mg, 2.60 mmol) were dissoved in THF/H_2O (10 mL, *v*/*v*, 3/1). The mixture was stirred refluxed under argon for 8 h. Water and chloroform were then added. The organic phase was washed with 0.2 M phosphoric acid aqueous solution and water in turn, and then dried over anhydrous sodium sulfate. After removing the solvent under reduced pressure, the crude product was purified by column chromatography (chloroform/methanol, *v*/*v*, 20/1) on silica gel to yield a black solid as the final product **SC-2** (306 mg, 76% yield). Melting point: 205–208 °C. ^{1}H NMR (400 MHz, THF-d_8) δ: 8.89–8.81 (m, 1H), 8.75–8.66 (m, 2H), 8.18–8.17 (m, 5H), 8.10–8.03 (m, 1H), 7.97–7.86 (m, 3H), 7.79–7.69 (m, 2H), 7.52 (d, *J* = 8.4 Hz, 2H), 7.15 (d, *J* = 8.8 Hz, 4H), 7.09 (d, *J* = 8.4 Hz, 2H), 6.89 (d, *J* = 8.8 Hz, 4H), 4.62–4.45 (m, 2H), 3.96 (t, *J* = 6.2 Hz, 4H), 2.10–2.00 (m, 1H), 1.82–1.72 (m, 4H), 1.52–1.49 (m, 4H), 1.38–1.37 (m, 12H), 1.29 (br, 6H), 1.16–1.13 (m, 14H), 0.95–0.87 (m, 6H), 0.78–0.75 (m, 6H). ^{13}C NMR (100 MHz, THF-d_8) δ: 167.47, 157.22, 156.13, 153.74, 150.40, 141.77, 140.42, 133.31, 132.99, 132.38, 131.47, 130.40, 129.70, 128.94, 128.04, 119.03, 118.29, 115.97, 113.75, 98.31, 85.28, 68.58, 36.04, 33.68, 32.65, 32.37, 30.50, 30.43, 30.33, 30.26, 30.24, 30.09, 27.82, 26.53, 26.23, 23.33, 17.02, 14.27, 14.23. HR-MS (MALDI-TOF) *m*/*z* calcd. for ($C_{81}H_{86}N_4O_4S$): 1210.63698. Found: 1210.63725. Anal. Calcd. for $C_{81}H_{86}N_4O_4S$: C, 80.29; H, 7.15; N, 4.62. Found: C, 80.27; H, 7.13; N, 4.65%.

N,N-Bis(2',4'-bis(hexyloxy)-[1,1'-biphenyl]-4-yl)-1-(2-hexyldecyl)-1H-phenanthro[1,10,9,8-cdefg]carbazol-3-amine: To a dried Schlenk tube bis(2',4'-bis(hexyloxy)-[1,1'-biphenyl]-4-yl)amine (1.44 g, 2.00 mmol), 3-bromo-1-(2-hexyldecyl)-1*H*-phenanthro[1,10,9,8-*cdefg*]carbazole (1.14 g, 2.00 mmol), $Pd_2(dba)_3$ (82 mg, 0.09 mmol), RuPhos (84 mg, 0.18 mmol), NaO*t*-Bu (0.96 g, 10.00 mmol), and toluene (20 mL) were added in the nitrogen-filled glovebox. The reaction mixture was refluxed under argon for 24 h and then cooled to room temperature. Water was added to terminate the reaction. The resultant mixture was extracted three times with chloroform before the organic phase was washed with water and dried over anhydrous sodium sulfate. After solvent removal under reduced pressure, the residue was purified by column chromatography over silica gel with toluene/petroleum ether (*v*/*v*, 1/2) as eluent to afford a yellow oil as the desired product (1.84 g, 76% yield). ^{1}H NMR (400 MHz, THF-d_8) δ: 8.70–8.67 (m, 2H), 8.11–8.08 (m, 2H), 7.91-7.86 (m, 3H), 7.79–7.75 (m, 1H), 7.69–7.65 (m, 1H), 7.39 (d, J = 8.8 Hz, 4H), 7.21–7.18 (m, 6H), 6.55 (d, J = 2.3 Hz, 2H), 6.51–6.50 (m, 1H), 6.49–6.48 (m, 1H), 4.62 (d. J = 7.3 Hz, 2H), 3.96–3.91 (m, 8H), 2.25 (br, 1H), 1.50–1.49 (m, 4H), 1.41–1.35 (m, 18H), 1.29–1.26 (m, 12H), 1.17–1.15 (m, 18H), 0.93–0.90 (m, 7H), 0.84–0.81 (m, 6H), 0.79–0.75 (m, 6H). ^{13}C NMR (100 MHz, $CDCl_3$) δ: 159.54, 157.17, 141.18, 138.08, 132.74, 131.10, 130.96, 130.87, 130.17, 129.25, 128.83, 128.44, 128.01, 127.88, 125.51, 124.95, 124.85, 123.45, 121.22, 121.11, 116.11, 105.49, 104.43, 100.68, 68.61, 68.29, 56.12, 50.42, 40.18, 32.08, 32.05, 31.94, 31.83, 31.66, 30.09, 29.79, 29.67, 29.53, 29.42, 29.27, 26.70, 25.98, 25.92, 22.83, 22.80, 22.74, 14.25, 14.23, 14.20. HR-MS (MALDI-TOF) *m*/*z* calcd. for ($C_{84}H_{108}N_2O_4$): 1208.83091. Found: 1208.83052. Anal. Calcd. for $C_{84}H_{108}N_2O_4$: C, 83.40; H, 9.00; N, 2.32. Found: C, 83.42; H, 8.89; N, 2.34%.

*4-(7-((10-(Bis(2',4'-bis(hexyloxy)-[1,1'-biphenyl]-4-yl)amino)-1-(2-hexyldecyl)-1H-phenanthro[1,10,9,8-cdefg]carbazol-3-yl)ethynyl)benzo[c][1,2,5]thiadiazol-4-yl)benzoic acid (**SC-3**)*: In a three-neck round bottom flask, *N*,*N*-bis(2',4'-bis(hexyloxy)-[1,1'-biphenyl]-4-yl)-1-(2-hexyldecyl)-1*H*-phenanthro[1,10,9,8-*cdefg*]carbazol-3-amine (604 mg, 0.50 mmol) was dissoved with THF (40 mL). The solution was cooled to –10 ^{o}C by use of an ice salt bath before the dropwise addition of NBS (89 mg, 0.50 mmol) in THF (10 mL). The reaction mixture was stirred at –10 ^{o}C for 0.5 h. Water was then added to terminate the reaction and the mixture was extracted three times with chloroform. The organic phase was washed with water and then dried over anhydrous sodium sulfate. After solvent removal under reduced pressure, the residue was purified by column chromatography (toluene/petroleum ether 60–90 °C, *v*/*v*, 1/50) on silica gel to yield a yellow oil as the desired product *N*,*N*-bis(2',4'-bis(hexyloxy)-[1,1'-biphenyl]-4-yl)-10-bromo-1-(2-hexyldecyl)-1*H*-phenanthro[1,10,9,8-*cdefg*]carbazol-3-amine. Then, to a dried Schlenk tube were added *N*,*N*-bis(2',4'-bis(hexyloxy)-[1,1'-biphenyl]-4-yl)-10-bromo-1-(2-hexyldecyl)-1*H*-phenanthro[1,10,9,8-*cdefg*]carbazol-3-amine, butyl 4-(7-ethynylbenzo[*c*][1,2,5]thiadiazol-4-yl)benzoate (200 mg, 0.58 mmol), $Pd_2(dba)_3$ (18 mg, 0.02 mmol), P(*t*-Bu)$_3$ (0.046 mL, 0.02 mmol, 10 wt% in toluene), Cs_2CO_3 (112 mg, 0.34 mmol), and dioxane (15 mL) in a nitrogen-filled glovebox. The reaction mixture was refluxed under argon overnight. Water was added and the mixture was extracted three times with chloroform. The organic phase was washed with water and then dried over anhydrous sodium sulfate. After solvent removal under reduced pressure, the residue was purified by column chromatography (toluene/petroleum ether 60–90 °C, *v*/*v*, 1/1) on silica gel to yield a red solid as the desired butyl ester. Then in a three-neck round bottom flask, butyl ester and KOH (152 mg, 2.61 mmol) were dissoved in THF/H_2O (12 mL, *v*/*v*, 3/1). The mixture was stirred at reflux overnight. Water and chloroform were then added. The organic phase was washed with 0.2 M phosphoric acid aqueous solution and water in turn, and then dried over anhydrous sodium sulfate. After removing the solvent under reduced pressure, the crude product was purified by column chromatography (chloroform/methanol, *v*/*v*, 20/1) on silica gel to yield a black solid as the final product **SC-3** (528 mg, 71% yield). Melting point: 178−191 °C. ^{1}H NMR (500 MHz, THF-d_8) δ: 8.90 (d, J = 8.2 Hz, 1H), 8.78 (d, J = 7.6 Hz, 1H), 8.73 (d, J = 7.6 Hz, 1H), 8.29 (s, 1H), 8.23–8.19 (m, 4H), 8.11 (d, J = 8.3 Hz, 1H), 8.06 (d, J = 7.3 Hz, 1H), 8.00–7.96 (m, 2H), 7.91 (s, 1H), 7.72–7.69 (m, 1H), 7.42 (d, J = 8.7 Hz, 4H), 7.23–7.19 (m, 6H), 6.55 (d, J = 2.3 Hz, 2H), 6.51 (d, J = 2.3 Hz, 1H), 6.50 (d, J = 2.3 Hz, 1H), 4.65 (d, J = 7.3 Hz, 2H), 3.97–3.93 (m, 8H), 2.28 (br, 1H), 1.79–1.74 (m, 4H), 1.50–1.47 (m, 4H), 1.43–1.34 (m, 20H), 1.29–1.26 (m, 6H), 1.18–1.12 (m, 16H), 0.93–0.90 (m, 9H), 0.84–0.81 (m, 6H), 0.77–0.74 (m, 6H). ^{13}C NMR (150 MHz, THF-d_8) δ: 167.87, 160.77, 158.15, 156.74, 154.25, 148.09, 143.86, 142.13, 135.47, 133.85, 133.69, 133.32, 132.89, 132.76, 131.78, 131.65, 131.52, 131.47, 131.02, 130.83, 130.79, 130.13, 129.75, 129.46, 128.95, 126.56, 125.96, 125.38, 125.04, 124.56, 124.06, 122.64, 122.44, 122.12, 119.49, 119.34, 118.59, 116.78, 116.71, 116.60, 106.37, 101.32, 98.55, 91.05, 69.16, 68.70, 50.79, 41.05, 40.08, 32.98, 32.89, 32.82, 32.77, 32.60, 31.55, 31.08, 30.80, 30.78, 30.62, 30.47, 30.27, 30.04, 27.50, 26.91, 26.86, 23.70, 23.63, 14.58. HR-MS (MALDI-TOF) *m*/*z* calcd. for ($C_{99}H_{114}N_4O_6S$): 1487.84926. Found: 1487.84911. Anal. Calcd. for $C_{99}H_{114}N_4O_6S$: C,79.91; H, 7.72; N, 3.77. Found: C, 79.93; H, 7.70; N, 3.76%.

References

S1 M. Zhang, Y. Wang, M. Xu, W. Ma, R. Li and P. Wang, *Energy Environ. Sci.*, 2013, **6**, 2944.

S2 L. Yang, Y. Ren, Z. Yao, C. Yan, W. Ma and P. Wang, *J. Phys. Chem. C*, 2015, **119**, 980.

S3 Y. Ren, Y. Li, S. Chen, J. Liu, J. Zhang and P. Wang, *Energy Environ. Sci.*, 2016, **9**, 1390.

S4 J.-H. Yum, T. W. Holcombe, Y. Kim, J. Yoon, K. Rakstys, M. K. Nazeeruddin and M. Grätzel, *Chem. Commun.*, 2012, **48**, 10727.

S5 Y. Li and Z. Wang, *Org. Lett.*, 2009, **11**, 1385.

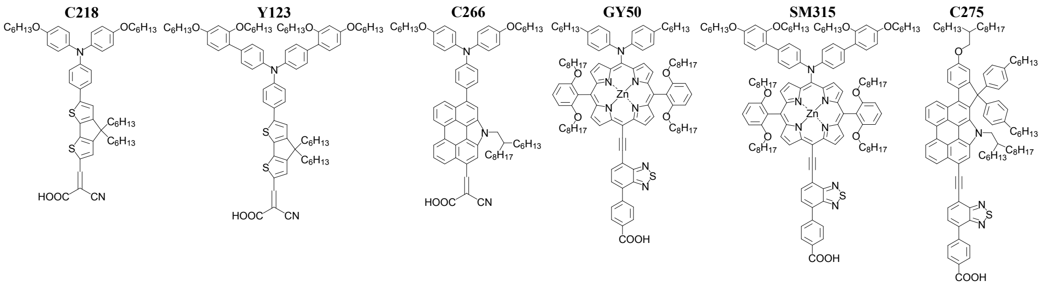

Fig. S1. Molecular structures of **C218**, **Y123**, **C266**, **GY50**, **SM315**, and **C275**.

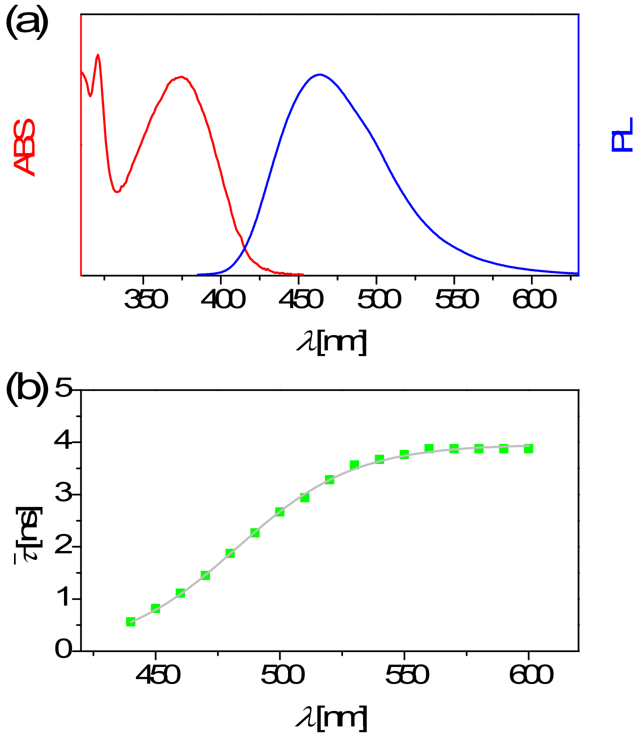

Fig. S2. (a) Electronic absorption and PL spectra of 50 μM of EBTBA in THF. (b) Wavelength-dependent average time constants ($\bar{\tau}$) for EBTBA dissolved in THF. The solid line was shown as a guide to the eyes.

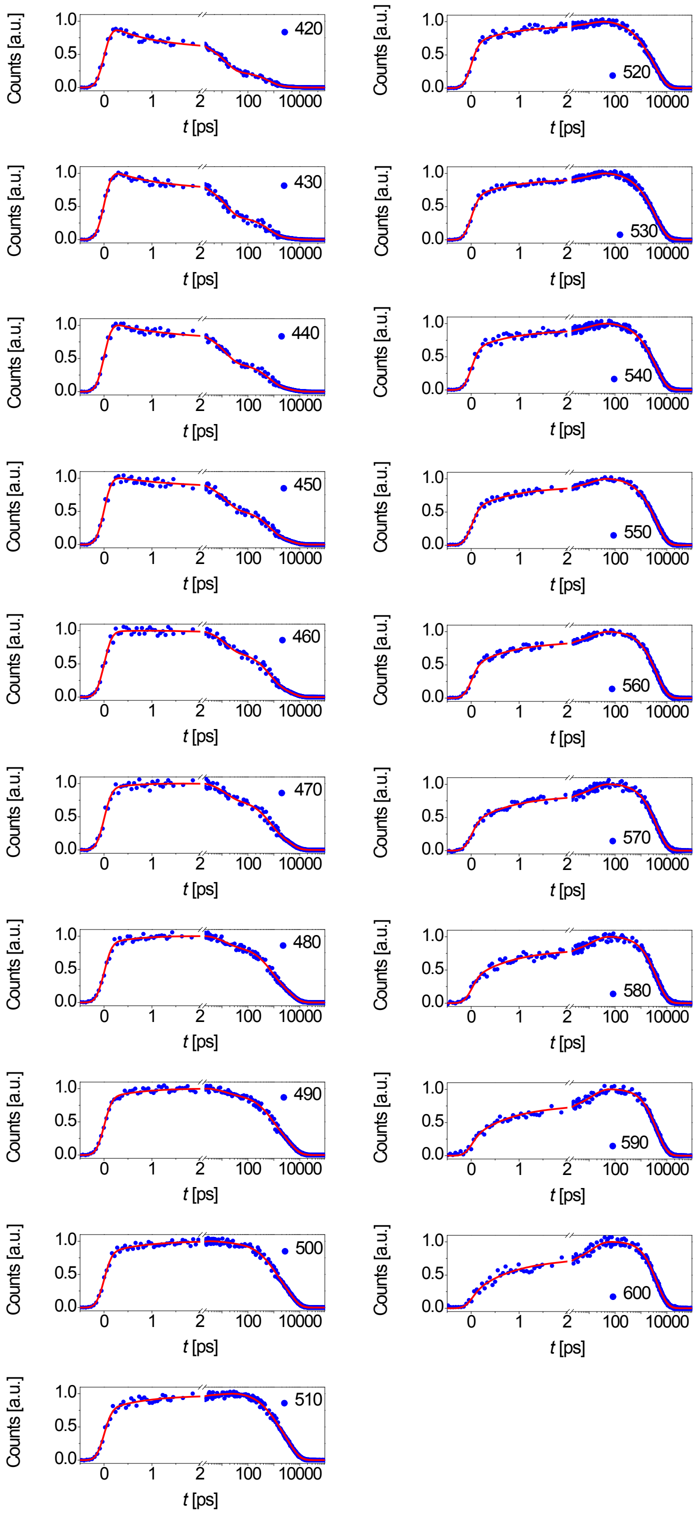

Fig. S3. PL traces (blue dots) of EBTBA in THF (50 μM) probed at a series of wavelengths. Note that PL intensities at different wavelengths have been normalized. The red solid lines are fittings via eqn.: $I_{\mathrm{PL}} = I_0 + \sum_{i=1}^{4} A_i \exp(-t/\tau_i) \otimes \mathrm{IRF}$. Excitation wavelength: 380 nm.

Table S1. Time constants and amplitudes employed to fit PL traces for EBTBA in THF [a]

λ [nm]	A_1	τ_1 [ps]	A_2	τ_2 [ps]	A_3	τ_3 [ps]	A_4	τ_4 [ps]	$\bar{\tau}$ [ps]
420	0.32±0.020	0.75±0.04	0.43±0.022	13.5±1.1	0.21±0.014	632.0±29.2	0.03±0.002	3875.0±56.4	257.6±8.1
430	0.23±0.013	0.75±0.04	0.45±0.025	13.5±1.1	0.26±0.016	632.0±29.2	0.05±0.004	3875.0±56.4	384.3±15.3
440	0.18±0.012	0.75±0.04	0.42±0.022	13.5±1.1	0.30±0.019	632.0±29.2	0.10±0.006	3875.0±56.4	562.2±24.2
450	0.11±0.007	0.75±0.04	0.39±0.024	13.5±1.1	0.35±0.017	632.0±29.2	0.15±0.011	3875.0±56.4	815.9±43.6
460	-0.06±0.003	0.75±0.04	0.34±0.027	13.5±1.1	0.45±0.020	632.0±29.2	0.21±0.014	3875.0±56.4	1111.4±55.6
470	-0.12±0.009	0.75±0.04	0.27±0.019	13.5±1.1	0.43±0.019	632.0±29.2	0.30±0.017	3875.0±56.4	1449.0±68.9
480	-0.15±0.011	0.75±0.04	0.18±0.012	13.5±1.1	0.40±0.021	632.0±29.2	0.42±0.020	3875.0±56.4	1872.8±78.2
490	-0.18±0.012	0.75±0.04	0.11±0.007	13.5±1.1	0.37±0.019	632.0±29.2	0.52±0.023	3875.0±56.4	2267.1±88.5
500	-0.21±0.017	0.75±0.04	0.03±0.001	13.5±1.1	0.34±0.021	632.0±29.2	0.63±0.027	3875.0±56.4	2663.8±107.9
510	-0.23±0.020	0.75±0.04	-0.05±0.003	13.5±1.1	0.29±0.025	632.0±29.2	0.71±0.030	3875.0±56.4	2937.3±117.5
520	-0.27±0.019	0.75±0.04	-0.10±0.005	13.5±1.1	0.18±0.011	632.0±29.2	0.82±0.032	3875.0±56.4	3281.8±123.3
530	-0.27±0.021	0.75±0.04	-0.12±0.007	13.5±1.1	0.10±0.007	632.0±29.2	0.90±0.033	3875.0±56.4	3566.0±129.5
540	-0.29±0.022	0.75±0.04	-0.13±0.005	13.5±1.1	0.06±0.003	632.0±29.2	0.94±0.027	3875.0±56.4	3672.3±108.4
550	-0.33±0.025	0.75±0.04	-0.16±0.012	13.5±1.1	0.03±0.001	632.0±29.2	0.97±0.029	3875.0±56.4	3763.7±115.2
560	-0.34±0.021	0.75±0.04	-0.19±0.014	13.5±1.1	-0.03±0.002	632.0±29.2	1.00±0.032	3875.0±56.4	3875.0±125.7
570	-0.37±0.022	0.75±0.04	-0.21±0.017	13.5±1.1	-0.06±0.003	632.0±29.2	1.00±0.031	3875.0±56.4	3875.0±122.6
580	-0.39±0.018	0.75±0.04	-0.23±0.015	13.5±1.1	-0.07±0.004	632.0±29.2	1.00±0.035	3875.0±56.4	3875.0±140.3
590	-0.42±0.031	0.75±0.04	-0.26±0.021	13.5±1.1	-0.10±0.006	632.0±29.2	1.00±0.032	3875.0±56.4	3875.0±127.3
600	-0.44±0.032	0.75±0.04	-0.27±0.022	13.5±1.1	-0.12±0.010	632.0±29.2	1.00±0.037	3875.0±56.4	3875.0±152.3

[a] The average lifetime of PL at a certain wavelength was calculated according to eqn.: $\bar{\tau} = \sum_{i=1}^{4} A_i \tau_i / \sum_{i=1}^{4} A_i (A_i > 0)$.

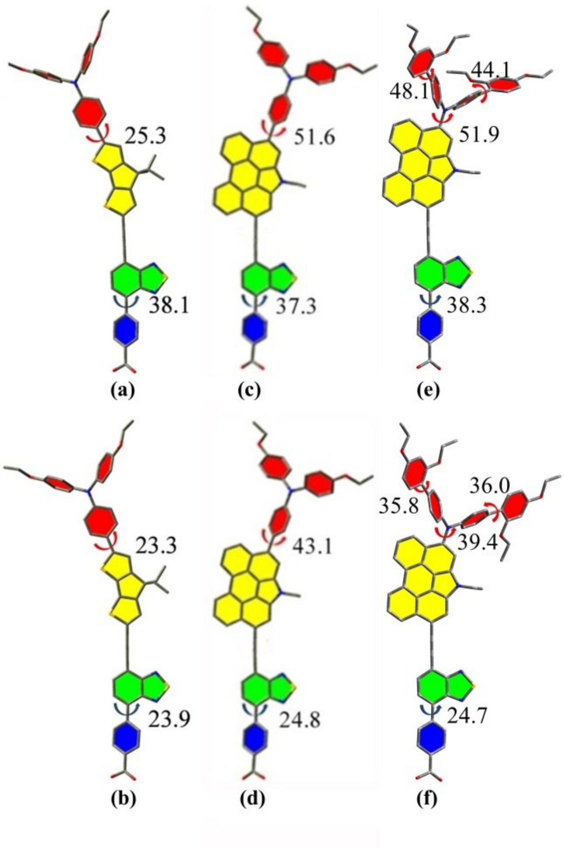

Fig. S4. Optimized geometries of the ground singlet states (S_0) and first equilibrium excited singlet states (S_1^{eq}) with THF as solvent: (a) S_0 of **SC-1**, (b) S_1^{eq} of **SC-1**, (c) S_0 of **SC-2**, (d) S_1^{eq} of **SC-2**, (e) S_0 of **SC-3**, and (f) S_1^{eq} of **SC-3**. The large aliphatic chains were replaced with ethyl to improve the computational efficiency. Dihedral angles are included on the side of a molecular skeleton, and are evidently distinct at the S_1^{vert} and S_1^{eq} states. Aromatic rings are filled with various colors for clarity of presentation.

Fig. S5. PL traces (blue dots) of **SC-1** in THF (50 μM) probed at a series of wavelengths. Note that PL intensities at different wavelengths have been normalized. The red solid lines are fittings via eqn.: $I_{\mathrm{PL}} = I_0 + \sum_{i=1}^{4} A_i \exp(-t/\tau_i) \otimes \mathrm{IRF}$. Excitation wavelength: 490 nm.

Table S2. Time constants and amplitudes employed to fit PL traces for **SC-1** in THF [a]

λ [nm]	A_1	τ_1 [ps]	A_2	τ_2 [ps]	A_3	τ_3 [ps]	A_4	τ_4 [ps]	$\bar{\tau}$ [ps]
580	0.71±0.035	0.39±0.04	0.25±0.019	1.1±0.08	0.04±0.002	5.2±0.3	0	86.6±2.2	0.76±0.01
590	0.62±0.030	0.39±0.04	0.34±0.015	1.1±0.08	0.04±0.003	5.2±0.3	0	86.6±2.2	1.0±0.02
600	0.58±0.032	0.39±0.04	0.38±0.030	1.1±0.08	0.04±0.003	5.2±0.3	0	86.6±2.2	1.2±0.02
610	0.52±0.038	0.39±0.04	0.42±0.027	1.1±0.08	0.05±0.004	5.2±0.3	0.01±0.001	86.6±2.2	1.5±0.1
620	0.36±0.028	0.39±0.04	0.57±0.032	1.1±0.08	0.06±0.004	5.2±0.3	0.01±0.001	86.6±2.2	2.1±0.1
630	0.24±0.019	0.39±0.04	0.68±0.040	1.1±0.08	0.06±0.003	5.2±0.3	0.02±0.001	86.6±2.2	2.9±0.1
640	0.11±0.008	0.39±0.04	0.79±0.042	1.1±0.08	0.07±0.002	5.2±0.3	0.03±0.002	86.6±2.2	3.5±0.2
650	0.04±0.003	0.39±0.04	0.84±0.041	1.1±0.08	0.08±0.005	5.2±0.3	0.04±0.003	86.6±2.2	4.6±0.3
660	-0.10±0.008	0.39±0.04	0.87±0.032	1.1±0.08	0.08±0.003	5.2±0.3	0.05±0.003	86.6±2.2	6.0±0.3
670	-0.19±0.012	0.39±0.04	0.84±0.038	1.1±0.08	0.09±0.003	5.2±0.3	0.07±0.004	86.6±2.2	7.3±0.4
680	-0.24±0.017	0.39±0.04	0.81±0.036	1.1±0.08	0.10±0.007	5.2±0.3	0.09±0.006	86.6±2.2	9.6±0.6
690	-0.30±0.021	0.39±0.04	0.78±0.032	1.1±0.08	0.10±0.005	5.2±0.3	0.12±0.008	86.6±2.2	11.6±0.7
700	-0.34±0.021	0.39±0.04	0.73±0.042	1.1±0.08	0.12±0.010	5.2±0.3	0.15±0.010	86.6±2.2	14.4±0.9
710	-0.39±0.022	0.39±0.04	0.67±0.032	1.1±0.08	0.14±0.012	5.2±0.3	0.19±0.014	86.6±2.2	18.1±1.3
720	-0.45±0.032	0.39±0.04	0.58±0.038	1.1±0.08	0.18±0.012	5.2±0.3	0.24±0.020	86.6±2.2	22.3±1.8
730	-0.45±0.029	0.39±0.04	0.48±0.035	1.1±0.08	0.23±0.016	5.2±0.3	0.29±0.021	86.6±2.2	26.1±2.0
740	-0.45±0。30	0.39±0.04	0.42±0.036	1.1±0.08	0.26±0.016	5.2±0.3	0.32±0.024	86.6±2.2	29.9±2.2
750	-0.46±0.031	0.39±0.04	0.33±0.028	1.1±0.08	0.28±0.021	5.2±0.3	0.39±0.023	86.6±2.2	35.7±2.2
760	-0.47±0.027	0.39±0.04	0.23±0.019	1.1±0.08	0.32±0.020	5.2±0.3	0.45±0.030	86.6±2.2	40.7±2.8
770	-0.47±0.025	0.39±0.04	0.15±0.012	1.1±0.08	0.32±0.024	5.2±0.3	0.53±0.032	86.6±2.2	47.4±3.0
830	-0.47±0.029	0.39±0.04	-0.22±0.017	1.1±0.08	0.12±0.010	5.2±0.3	0.88±0.038	86.6±2.2	76.5±3.4
840	-0.48±0.031	0.39±0.04	-0.24±0.021	1.1±0.08	0.07±0.005	5.2±0.3	0.93±0.043	86.6±2.2	81.1±3.8
850	-0.50±0.034	0.39±0.04	-0.28±0.020	1.1±0.08	0.03±0.002	5.2±0.3	0.97±0.046	86.6±2.2	84.2±4.1
860	-0.50±0.032	0.39±0.04	-0.32±0.021	1.1±0.08	-0.07±0.003	5.2±0.3	1.00±0.041	86.6±2.2	86.6±3.7
870	-0.51±0.034	0.39±0.04	-0.34±0.022	1.1±0.08	-0.08±0.005	5.2±0.3	1.00±0.045	86.6±2.2	86.6±4.0
880	-0.51±0.039	0.39±0.04	-0.35±0.019	1.1±0.08	-0.10±0.007	5.2±0.3	1.00±0.039	86.6±2.2	86.6±3.5
890	-0.51±0.028	0.39±0.04	-0.35±0.021	1.1±0.08	-0.10±0.008	5.2±0.3	1.00±0.046	86.6±2.2	86.6±4.1
900	-0.51±0.026	0.39±0.04	-0.35±0.023	1.1±0.08	-0.10±0.006	5.2±0.3	1.00±0.043	86.6±2.2	86.6±3.9
910	-0.51±0.027	0.39±0.04	-0.35±0.027	1.1±0.08	-0.10±0.006	5.2±0.3	1.00±0.040	86.6±2.2	86.6±3.6

[a] The average lifetime of PL at a certain wavelength was calculated according to eqn.: $\bar{\tau} = \sum_{i=1}^{4} A_i \tau_i \, / \sum_{i=1}^{4} A_i \, (A_i > 0)$.

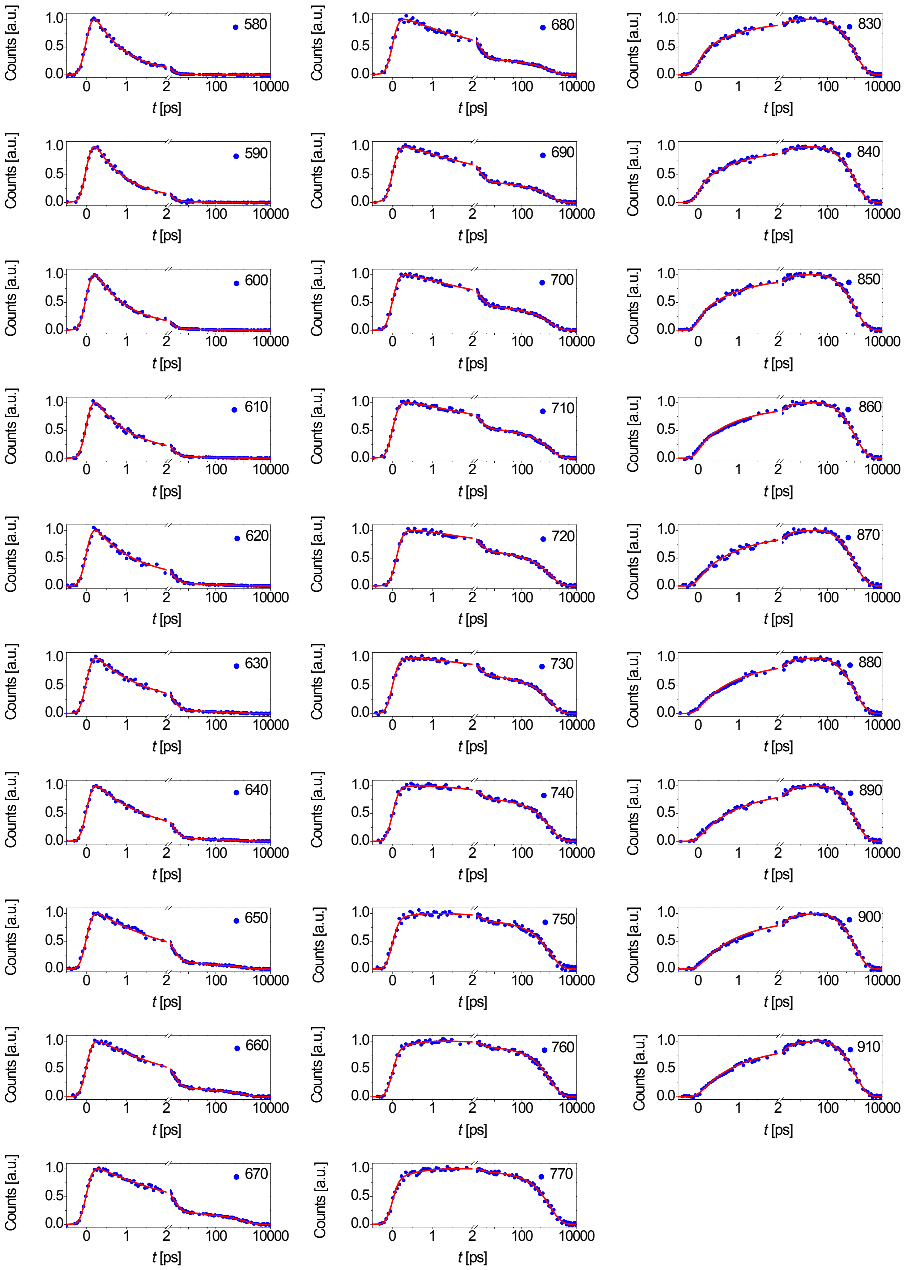

Fig. S6. PL traces (blue dots) of **SC-2** in THF (50 μM) probed at a series of wavelengths. Note that PL intensities at different wavelengths have been normalized. The red solid lines are fittings via eqn.: $I_{\mathrm{PL}} = I_0 + \sum_{i=1}^{4} A_i \exp(-t/\tau_i) \otimes \mathrm{IRF}$. Excitation wavelength: 490 nm.

Table S3. Time constants and amplitudes employed to fit PL traces for **SC-2** in THF [a]

λ [nm]	A_1	τ_1 [ps]	A_2	τ_2 [ps]	A_3	τ_3 [ps]	A_4	τ_4 [ps]	$\bar{\tau}$ [ps]
580	0.90±0.045	0.74±0.04	0.09±0.004	1.8±0.2	0.01±0.001	35.8±1.1	0	1049.0±19.7	1.5±0.04
590	0.84±0.043	0.74±0.04	0.15±0.012	1.8±0.2	0.01±0.001	35.8±1.1	0	1049.0±19.7	3.0±0.04
600	0.82±0.040	0.74±0.04	0.17±0.017	1.8±0.2	0.01±0.001	35.8±1.1	0	1049.0±19.7	5.9±0.04
610	0.65±0.038	0.74±0.04	0.32±0.015	1.8±0.2	0.02±0.001	35.8±1.1	0.01±0.001	1049.0±19.7	9.9±1.1
620	0.49±0.037	0.74±0.04	0.47±0.021	1.8±0.2	0.02±0.001	35.8±1.1	0.02±0.001	1049.0±19.7	18.4±1.1
630	0.24±0.021	0.74±0.04	0.70±0.023	1.8±0.2	0.03±0.002	35.8±1.1	0.03±0.002	1049.0±19.7	28.7±2.2
640	0.10±0.007	0.74±0.04	0.83±0.035	1.8±0.2	0.03±0.001	35.8±1.1	0.04±0.003	1049.0±19.7	45.3±3.2
650	-0.11±0.005	0.74±0.04	0.90±0.043	1.8±0.2	0.04±0.003	35.8±1.1	0.06±0.004	1049.0±19.7	67.5±4.3
660	-0.18±0.012	0.74±0.04	0.87±0.034	1.8±0.2	0.04±0.002	35.8±1.1	0.09±0.005	1049.0±19.7	94.6±5.3
670	-0.21±0.015	0.74±0.04	0.83±0.044	1.8±0.2	0.04±0.002	35.8±1.1	0.13±0.007	1049.0±19.7	135.5±7.4
680	-0.24±0.020	0.74±0.04	0.79±0.032	1.8±0.2	0.04±0.004	35.8±1.1	0.17±0.012	1049.0±19.7	181.0±12.7
690	-0.25±0.018	0.74±0.04	0.73±0.039	1.8±0.2	0.04±0.003	35.8±1.1	0.23±0.016	1049.0±19.7	240.7±16.9
700	-0.27±0.016	0.74±0.04	0.69±0.043	1.8±0.2	0.04±0.002	35.8±1.1	0.27±0.020	1049.0±19.7	285.9±21.1
710	-0.28±0.019	0.74±0.04	0.61±0.032	1.8±0.2	0.05±0.003	35.8±1.1	0.34±0.026	1049.0±19.7	358.3±27.4
720	-0.29±0.021	0.74±0.04	0.55±0.037	1.8±0.2	0.05±0.004	35.8±1.1	0.40±0.028	1049.0±19.7	424.3±29.5
730	-0.31±0.020	0.74±0.04	0.50±0.038	1.8±0.2	0.05±0.002	35.8±1.1	0.45±0.030	1049.0±19.7	474.4±31.5
740	-0.32±0.025	0.74±0.04	0.43±0.032	1.8±0.2	0.04±0.002	35.8±1.1	0.53±0.032	1049.0±19.7	554.9±33.6
750	-0.34±0.020	0.74±0.04	0.34±0.027	1.8±0.2	0.04±0.003	35.8±1.1	0.62±0.035	1049.0±19.7	657.3±36.8
760	-0.36±0.021	0.74±0.04	0.29±0.024	1.8±0.2	0.04±0.002	35.8±1.1	0.67±0.037	1049.0±19.7	703.5±38.9
770	-0.37±0.024	0.74±0.04	0.22±0.016	1.8±0.2	0.03±0.001	35.8±1.1	0.75±0.040	1049.0±19.7	789.8±42.0
830	-0.42±0.030	0.74±0.04	-0.21±0.015	1.8±0.2	-0.06±0.004	35.8±1.1	1.00±0.045	1049.0±19.7	1049.0±47.4
840	-0.42±0.031	0.74±0.04	-0.25±0.014	1.8±0.2	-0.07±0.005	35.8±1.1	1.00±0.043	1049.0±19.7	1049.0±45.3
850	-0.43±0.027	0.74±0.04	-0.27±0.020	1.8±0.2	-0.07±0.004	35.8±1.1	1.00±0.042	1049.0±19.7	1049.0±44.2
860	-0.44±0.029	0.74±0.04	-0.30±0.021	1.8±0.2	-0.09±0.005	35.8±1.1	1.00±0.040	1049.0±19.7	1049.0±42.1
870	-0.45±0.034	0.74±0.04	-0.34±0.024	1.8±0.2	-0.09±0.007	35.8±1.1	1.00±0.039	1049.0±19.7	1049.0±41.2
880	-0.46±0.036	0.74±0.04	-0.37±0.032	1.8±0.2	-0.10±0.008	35.8±1.1	1.00±0.038	1049.0±19.7	1049.0±40.2
890	-0.46±0.032	0.74±0.04	-0.40±0.032	1.8±0.2	-0.11±0.006	35.8±1.1	1.00±0.037	1049.0±19.7	1049.0±39.0
900	-0.46±0.031	0.74±0.04	-0.41±0.024	1.8±0.2	-0.12±0.010	35.8±1.1	1.00±0.040	1049.0±19.7	1049.0±42.3
910	-0.46±0.033	0.74±0.04	-0.41±0.028	1.8±0.2	-0.12±0.009	35.8±1.1	1.00±0.038	1049.0±19.7	1049.0±40.2

[a] The average lifetime of PL at a certain wavelength was calculated according to eqn.: $\bar{\tau} = \sum_{i=1}^{4} A_i \tau_i / \sum_{i=1}^{4} A_i (A_i > 0)$.

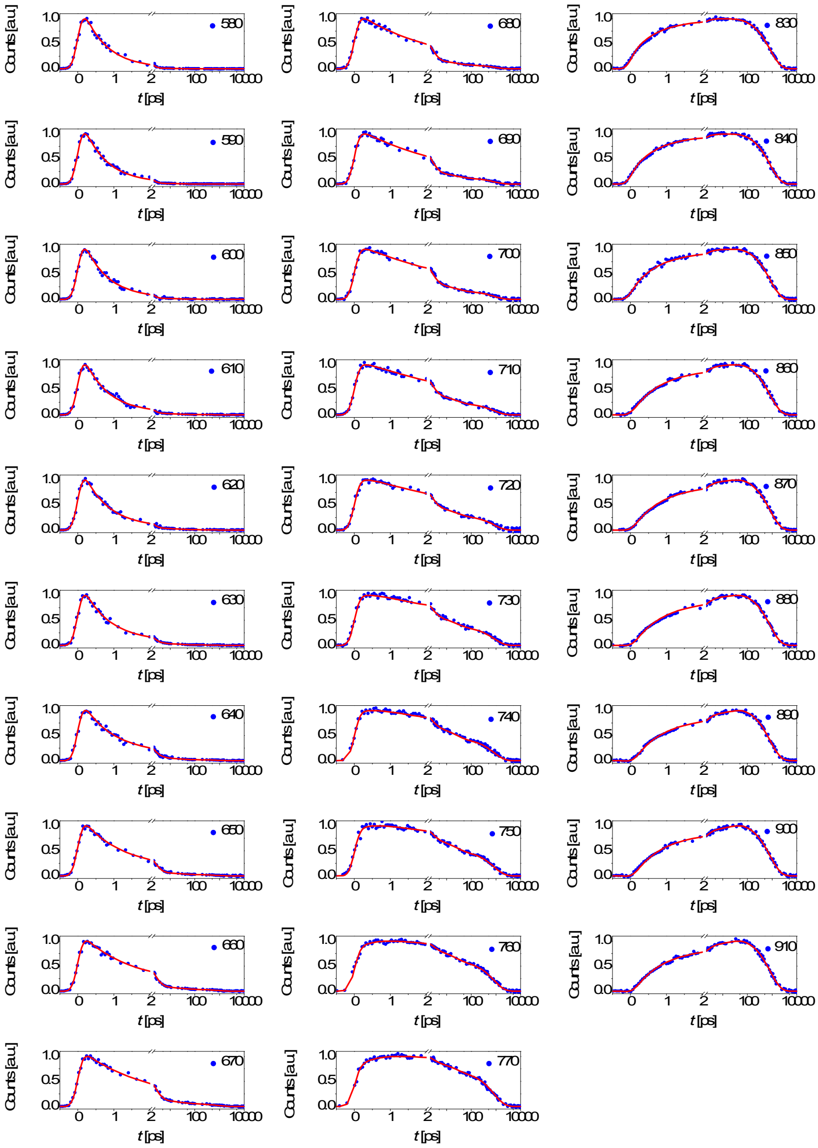

Fig. S7. PL traces (blue dots) of **SC-3** in THF (50 μM) probed at a series of wavelengths. Note that PL intensities at different wavelengths have been normalized. The red solid lines are fittings via eqn.: $I_{\mathrm{PL}} = I_0 + \sum_{i=1}^{4} A_i \exp(-t/\tau_i) \otimes \mathrm{IRF}$. Excitation wavelength: 490 nm.

Table S4. Time constants and amplitudes employed to fit PL traces for **SC-3** in THF [a]

λ	A_1	τ_1 [ps]	A_2	τ_2 [ps]	A_3	τ_3 [ps]	A_4	τ_4 [ps]	$\bar{\tau}$ [ps]
580	0.96±0.047	0.64±0.04	0.03±0.002	1.7±0.1	0.01±0.001	23.5±1.1	0	834.2±9.7	1.1±0.02
590	0.96±0.042	0.64±0.04	0.03±0.002	1.7±0.1	0.01±0.001	23.5±1.1	0	834.2±9.7	2.1±0.03
600	0.95±0.044	0.64±0.04	0.04±0.003	1.7±0.1	0.01±0.001	23.5±1.1	0	834.2±9.7	3.2±0.02
610	0.93±0.042	0.64±0.04	0.05±0.004	1.7±0.1	0.02±0.001	23.5±1.1	0	834.2±9.7	5.2±0.03
620	0.88±0.048	0.64±0.04	0.09±0.006	1.7±0.1	0.02±0.001	23.5±1.1	0.01±0.001	834.2±9.7	7.3±0.9
630	0.79±0.040	0.64±0.04	0.18±0.012	1.7±0.1	0.02±0.001	23.5±1.1	0.01±0.001	834.2±9.7	8.5±0.8
640	0.57±0.38	0.64±0.04	0.38±0.023	1.7±0.1	0.03±0.002	23.5±1.1	0.02±0.001	834.2±9.7	15.5±0.9
650	0.35±0.021	0.64±0.04	0.60±0.032	1.7±0.1	0.03±0.001	23.5±1.1	0.02±0.001	834.2±9.7	22.7±1.0
660	0.13±0.011	0.64±0.04	0.79±0.033	1.7±0.1	0.04±0.002	23.5±1.1	0.04±0.003	834.2±9.7	32.6±2.6
670	-0.06±0.003	0.64±0.04	0.88±0.035	1.7±0.1	0.06±0.003	23.5±1.1	0.06±0.003	834.2±9.7	45.4±2.8
680	-0.11±0.005	0.64±0.04	0.86±0.037	1.7±0.1	0.07±0.005	23.5±1.1	0.07±0.005	834.2±9.7	58.2±4.3
690	-0.19±0.012	0.64±0.04	0.83±0.038	1.7±0.1	0.08±0.004	23.5±1.1	0.09±0.004	834.2±9.7	81.5±3.5
700	-0.25±0.017	0.64±0.04	0.77±0.039	1.7±0.1	0.11±0.006	23.5±1.1	0.12±0.010	834.2±9.7	103.6±8.6
710	-0.27±0.021	0.64±0.04	0.71±0.032	1.7±0.1	0.13±0.008	23.5±1.1	0.16±0.012	834.2±9.7	140.7±10.3
720	-0.30±0.023	0.64±0.04	0.67±0.043	1.7±0.1	0.13±0.012	23.5±1.1	0.20±0.014	834.2±9.7	172.7±12.1
730	-0.32±0.025	0.64±0.04	0.59±0.032	1.7±0.1	0.15±0.012	23.5±1.1	0.26±0.016	834.2±9.7	225.0±13.8
740	-0.33±0.021	0.64±0.04	0.50±0.033	1.7±0.1	0.18±0.015	23.5±1.1	0.32±0.021	834.2±9.7	269.0±18.1
750	-0.36±0.022	0.64±0.04	0.46±0.029	1.7±0.1	0.18±0.014	23.5±1.1	0.36±0.024	834.2±9.7	302.6±20.6
760	-0.41±0.030	0.64±0.04	0.38±0.027	1.7±0.1	0.18±0.014	23.5±1.1	0.44±0.030	834.2±9.7	371.2±25.7
770	-0.44±0.031	0.64±0.04	0.31±0.025	1.7±0.1	0.16±0.012	23.5±1.1	0.53±0.033	834.2±9.7	443.6±28.1
830	-0.62±0.032	0.64±0.04	-0.12±0.010	1.7±0.1	-0.04±0.002	23.5±1.1	1.00±0.035	834.2±9.7	834.2±29.6
840	-0.62±0.035	0.64±0.04	-0.14±0.012	1.7±0.1	-0.06±0.005	23.5±1.1	1.00±0.042	834.2±9.7	834.2±35.7
850	-0.63±0.032	0.64±0.04	-0.18±0.013	1.7±0.1	-0.08±0.003	23.5±1.1	1.00±0.043	834.2±9.7	834.2±36.4
860	-0.63±0.037	0.64±0.04	-0.30±0.019	1.7±0.1	-0.10±0.007	23.5±1.1	1.00±0.045	834.2±9.7	834.2±38.1
870	-0.63±0.038	0.64±0.04	-0.31±0.021	1.7±0.1	-0.12±0.010	23.5±1.1	1.00±0.044	834.2±9.7	834.2±37.4
880	-0.63±0.029	0.64±0.04	-0.32±0.023	1.7±0.1	-0.14±0.011	23.5±1.1	1.00±0.042	834.2±9.7	834.2±35.7
890	-0.63±0.031	0.64±0.04	-0.32±0.024	1.7±0.1	-0.16±0.012	23.5±1.1	1.00±0.040	834.2±9.7	834.2±34.1
900	-0.63±0.033	0.64±0.04	-0.32±0.021	1.7±0.1	-0.16±0.012	23.5±1.1	1.00±0.039	834.2±9.7	834.2±33.1
910	-0.63±0.035	0.64±0.04	-0.32±0.020	1.7±0.1	-0.16±0.011	23.5±1.1	1.00±0.037	834.2±9.7	834.2±31.5

[a] The average lifetime of PL at a certain wavelength was calculated according to eqn.: $\bar{\tau} = \sum_{i=1}^{4} A_i \tau_i \,/\, \sum_{i=1}^{4} A_i (A_i > 0)$.

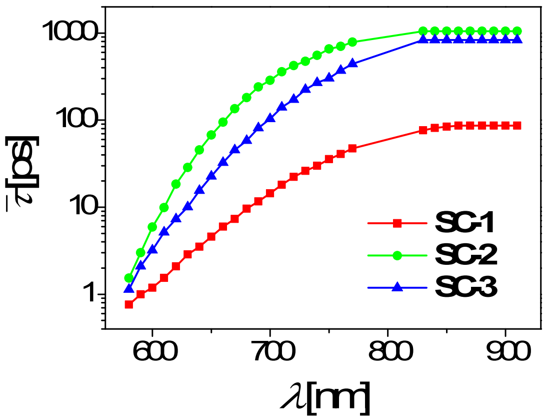

Fig. S8. Wavelength-dependent average time constants ($\bar{\tau}$) of **SC-1**, **SC-2**, and **SC-3** in THF.

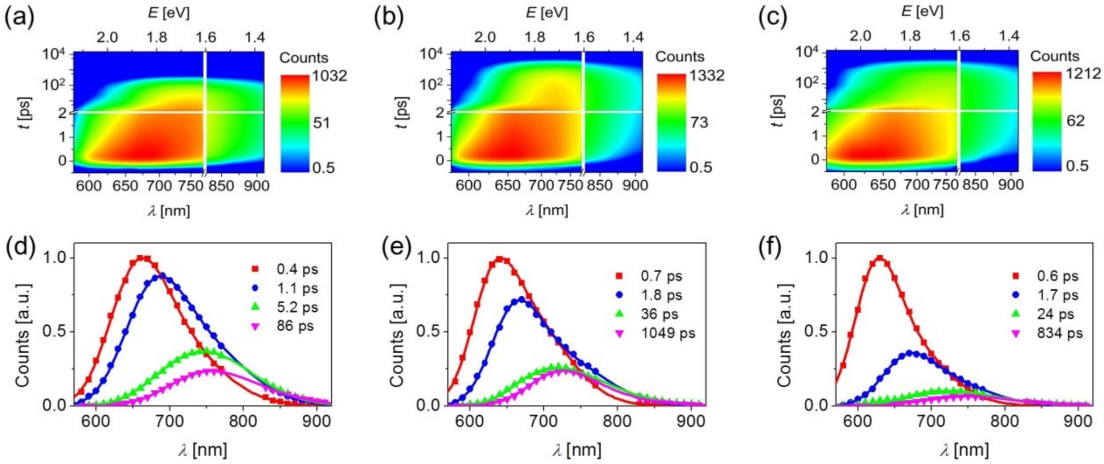

Fig. S9. (a–c) Contour plots of time-resolved PL (TRPL) spectra of (a) **SC-1** in THF, (b) **SC-2** in THF, and (c) **SC**-3 in THF, which were reconstructed based on the corresponding fitting curves in Fig. S5-S7 and static PL spectroscopies in Fig. 2c. (d-f) Evolution associated PL (EAPL) spectra of (d) **SC-1** in THF, (e) **SC-2** in THF, and (f) **SC-3** in THF. The solid lines are fitting lines with a lognormal function.

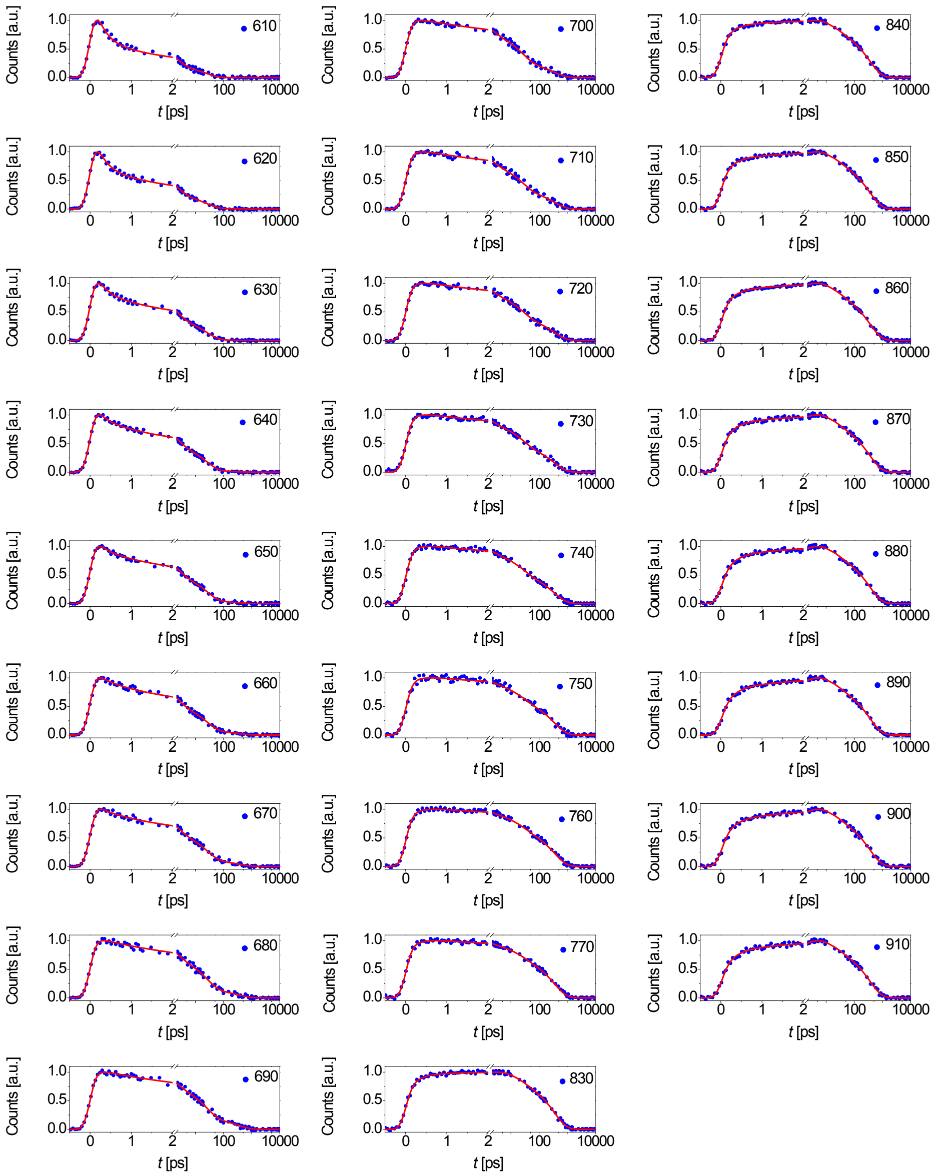

Fig. S10. PL traces (blue dots) of a **SC-1** grafted alumina film in contact with an electrolyte probed at a series of wavelengths. Note that PL intensities at different wavelengths have been normalized. The red solid lines are fittings via eqn.: $I_{\mathrm{PL}} = I_0 + \sum_{i=1}^{4} A_i \exp(-t/\tau_i) \otimes \mathrm{IRF}$. Excitation wavelength: 490 nm.

Table S5. Time constants and amplitudes employed to fit PL traces for a **SC-1** grafted alumina film in contact with an electrolyte [a]

λ [nm]	A_1	τ_1 [ps]	A_2	τ_2 [ps]	A_3	τ_3 [ps]	A_4	τ_4 [ps]	$\bar{\tau}$ [ps]
610	0.64±0.033	0.23±0.02	0.26±0.021	1.0±0.06	0.10±0.005	25.3±1.0	0	351.4±6.4	3.2±0.1
620	0.58±0.037	0.23±0.02	0.28±0.024	1.0±0.06	0.14±0.011	25.3±1.0	0	351.4±6.4	5.4±0.3
630	0.43±0.032	0.23±0.02	0.33±0.020	1.0±0.06	0.23±0.016	25.3±1.0	0.01±0.001	351.4±6.4	8.6±0.8
640	0.31±0.019	0.23±0.02	0.36±0.021	1.0±0.06	0.32±0.020	25.3±1.0	0.01±0.001	351.4±6.4	14.1±0.9
650	0.24±0.020	0.23±0.02	0.37±0.019	1.0±0.06	0.36±0.022	25.3±1.0	0.03±0.002	351.4±6.4	21.1±1.3
660	0.16±0.013	0.23±0.02	0.41±0.026	1.0±0.06	0.37±0.025	25.3±1.0	0.06±0.004	351.4±6.4	30.1±2.1
670	0.12±0.010	0.23±0.02	0.38±0.031	1.0±0.06	0.41±0.026	25.3±1.0	0.09±0.005	351.4±6.4	43.0±2.5
680	-0.09±0.007	0.23±0.02	0.36±0.027	1.0±0.06	0.51±0.033	25.3±1.0	0.13±0.011	351.4±6.4	58.4±4.8
690	-0.11±0.008	0.23±0.02	0.32±0.022	1.0±0.06	0.51±0.036	25.3±1.0	0.17±0.012	351.4±6.4	72.9±5.2
700	-0.15±0.011	0.23±0.02	0.30±0.031	1.0±0.06	0.47±0.032	25.3±1.0	0.23±0.017	351.4±6.4	94.8±6.9
710	-0.19±0.012	0.23±0.02	0.29±0.024	1.0±0.06	0.41±0.030	25.3±1.0	0.30±0.021	351.4±6.4	113.7±8.3
720	-0.21±0.015	0.23±0.02	0.26±0.022	1.0±0.06	0.39±0.028	25.3±1.0	0.35±0.024	351.4±6.4	134.7±9.3
730	-0.26±0.021	0.23±0.02	0.23±0.021	1.0±0.06	0.36±0.021	25.3±1.0	0.41±0.027	351.4±6.4	154.1±10.2
740	-0.29±0.023	0.23±0.02	0.19±0.015	1.0±0.06	0.34±0.020	25.3±1.0	0.47±0.030	351.4±6.4	173.6±11.3
750	-0.31±0.026	0.23±0.02	0.16±0.012	1.0±0.06	0.30±0.025	25.3±1.0	0.54±0.031	351.4±6.4	198.2±11.7
760	-0.34±0.030	0.23±0.02	0.14±0.011	1.0±0.06	0.27±0.016	25.3±1.0	0.59±0.037	351.4±6.4	215.9±13.7
770	-0.34±0.027	0.23±0.02	0.13±0.009	1.0±0.06	0.24±0.014	25.3±1.0	0.63±0.038	351.4±6.4	229.5±14.0
830	-0.39±0.025	0.23±0.02	-0.11±0.007	1.0±0.06	0.25±0.017	25.3±1.0	0.75±0.030	351.4±6.4	270.4±11.2
840	-0.40±0.027	0.23±0.02	-0.16±0.012	1.0±0.06	0.25±0.016	25.3±1.0	0.75±0.040	351.4±6.4	270.4±14.7
850	-0.42±0.030	0.23±0.02	-0.20±0.015	1.0±0.06	0.25±0.015	25.3±1.0	0.75±0.041	351.4±6.4	270.4±15.1
860	-0.43±0.032	0.23±0.02	-0.21±0.017	1.0±0.06	0.25±0.012	25.3±1.0	0.75±0.043	351.4±6.4	270.4±15.7
870	-0.47±0.033	0.23±0.02	-0.23±0.015	1.0±0.06	0.25±0.014	25.3±1.0	0.75±0.045	351.4±6.4	270.4±16.5
880	-0.49±0.035	0.23±0.02	-0.25±0.020	1.0±0.06	0.25±0.020	25.3±1.0	0.75±0.032	351.4±6.4	270.4±12.0
890	-0.49±0.029	0.23±0.02	-0.28±0.021	1.0±0.06	0.25±0.021	25.3±1.0	0.75±0.038	351.4±6.4	270.4±14.2
900	-0.49±0.037	0.23±0.02	-0.28±0.023	1.0±0.06	0.25±0.020	25.3±1.0	0.75±0.041	351.4±6.4	270.4±15.2
910	-0.49±0.032	0.23±0.02	-0.28±0.017	1.0±0.06	0.25±0.017	25.3±1.0	0.75±0.042	351.4±6.4	270.4±15.5

[a] The average lifetime of PL at a certain wavelength was calculated according to eqn.: $\bar{\tau} = \sum_{i=1}^{4} A_i \tau_i / \sum_{i=1}^{4} A_i (A_i > 0)$.

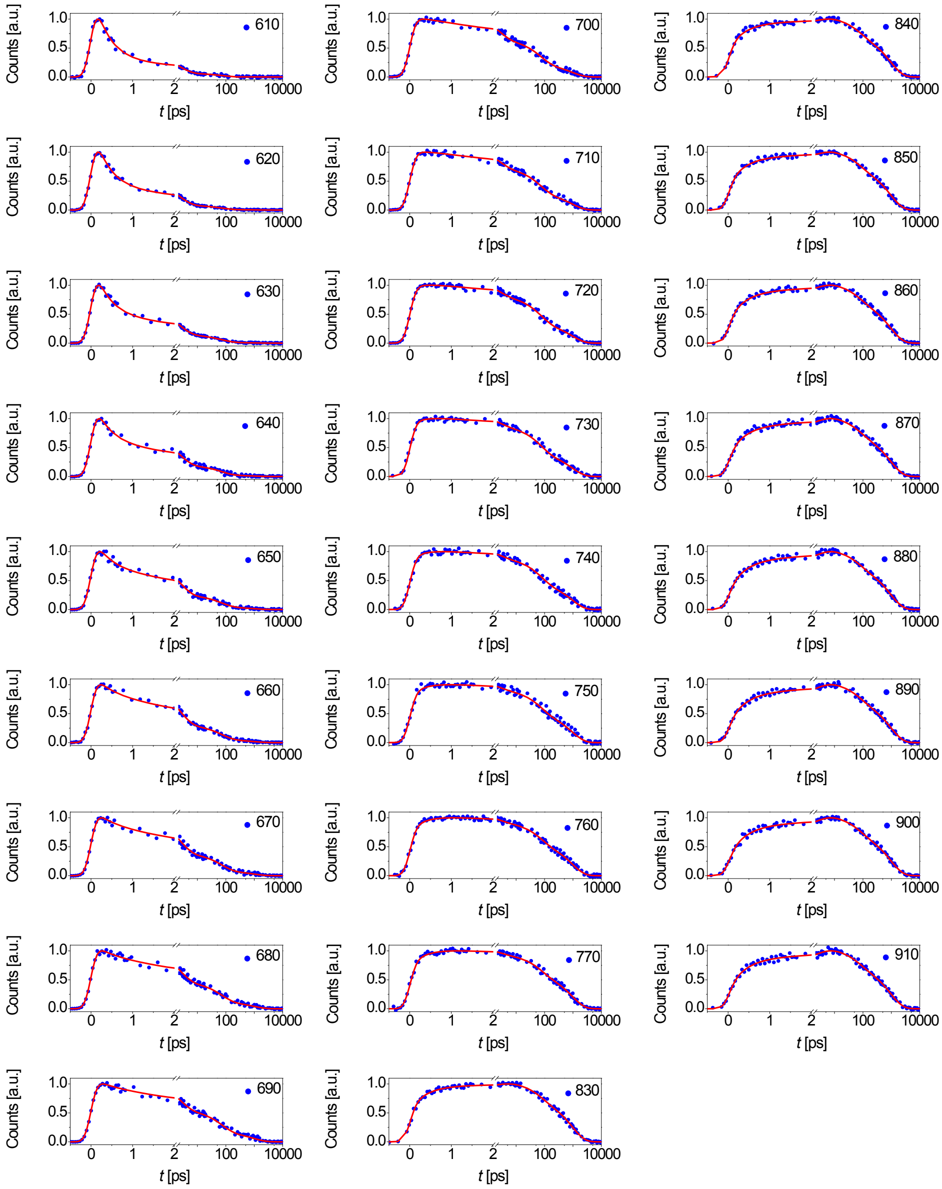

Fig. S11. PL traces (blue dots) of a **SC-2** grafted alumina film in contact with an electrolyte probed at a series of wavelengths. Note that PL intensities at different wavelengths have been normalized. The red solid lines are fittings via eqn.: $I_{PL} = I_0 + \sum_{i=1}^{4} A_i \exp(-t/\tau_i) \otimes \text{IRF}$. Excitation wavelength: 490 nm.

Table S5. Time constants and amplitudes employed to fit PL traces for a **SC-2** grafted alumina film in contact with an electrolyte [a]

λ [nm]	A_1	τ_1 [ps]	A_2	τ_2 [ps]	A_3	τ_3 [ps]	A_4	τ_4 [ps]	$\bar{\tau}$ [ps]
610	0.79±0.038	0.35±0.03	0.17±0.013	2.5±0.3	0.04±0.003	71.2±2.4	0	945±11.6	4.4±0.2
620	0.72±0.036	0.35±0.03	0.24±0.021	2.5±0.3	0.04±0.002	71.2±2.4	0	945±11.6	8.2±0.1
630	0.64±0.032	0.35±0.03	0.27±0.018	2.5±0.3	0.08±0.006	71.2±2.4	0.01±0.001	945±11.6	13.4±1.4
640	0.56±0.028	0.35±0.03	0.32±0.020	2.5±0.3	0.11±0.007	71.2±2.4	0.01±0.001	945±11.6	23.3±1.5
650	0.40±0.030	0.35±0.03	0.42±0.021	2.5±0.3	0.15±0.011	71.2±2.4	0.03±0.001	945±11.6	41.0±1.8
660	0.22±0.016	0.35±0.03	0.53±0.023	2.5±0.3	0.21±0.018	71.2±2.4	0.04±0.002	945±11.6	54.8±3.2
670	0.16±0.014	0.35±0.03	0.51±0.039	2.5±0.3	0.26±0.017	71.2±2.4	0.07±0.004	945±11.6	83.1±5.1
680	0.12±0.010	0.35±0.03	0.48±0.036	2.5±0.3	0.30±0.021	71.2±2.4	0.10±0.007	945±11.6	119.1±8.2
690	0.06±0.004	0.35±0.03	0.44±0.32	2.5±0.3	0.35±0.023	71.2±2.4	0.15±0.012	945±11.6	167.7±13.2
700	-0.06±0.005	0.35±0.03	0.40±0.027	2.5±0.3	0.40±0.027	71.2±2.4	0.20±0.017	945±11.6	219.6±18.2
710	-0.10±0.003	0.35±0.03	0.33±0.019	2.5±0.3	0.41±0.026	71.2±2.4	0.26±0.018	945±11.6	275.9±19.1
720	-0.14±0.012	0.35±0.03	0.25±0.012	2.5±0.3	0.44±0.029	71.2±2.4	0.31±0.021	945±11.6	324.8±22.2
730	-0.17±0.012	0.35±0.03	0.19±0.012	2.5±0.3	0.44±0.030	71.2±2.4	0.37±0.023	945±11.6	379.3±24.2
740	-0.21±0.017	0.35±0.03	0.17±0.011	2.5±0.3	0.41±0.032	71.2±2.4	0.42±0.028	945±11.6	422.9±29.1
750	-0.28±0.021	0.35±0.03	0.15±0.011	2.5±0.3	0.38±0.030	71.2±2.4	0.47±0.032	945±11.6	470.1±32.8
760	-0.31±0.025	0.35±0.03	0.14±0.010	2.5±0.3	0.35±0.028	71.2±2.4	0.51±0.035	945±11.6	508.5±35.5
770	-0.36±0.027	0.35±0.03	0.12±0.008	2.5±0.3	0.33±0.021	71.2±2.4	0.55±0.038	945±11.6	543.3±37.9
830	-0.42±0.030	0.35±0.03	-0.10±0.007	2.5±0.3	0.32±0.019	71.2±2.4	0.68±0.036	945±11.6	667.3±35.8
840	-0.46±0.032	0.35±0.03	-0.14±0.012	2.5±0.3	0.32±0.017	71.2±2.4	0.68±0.038	945±11.6	667.3±37.6
850	-0.48±0.033	0.35±0.03	-0.17±0.014	2.5±0.3	0.32±0.020	71.2±2.4	0.68±0.033	945±11.6	667.3±33.0
860	-0.50±0.036	0.35±0.03	-0.19±0.013	2.5±0.3	0.32±0.024	71.2±2.4	0.68±0.032	945±11.6	667.3±29.3
870	-0.51±0.037	0.35±0.03	-0.21±0.017	2.5±0.3	0.32±0.026	71.2±2.4	0.68±0.029	945±11.6	667.3±32.4
880	-0.52±0.035	0.35±0.03	-0.24±0.020	2.5±0.3	0.32±0.025	71.2±2.4	0.68±0.031	945±11.6	667.3±29.7
890	-0.52±0.032	0.35±0.03	-0.24±0.018	2.5±0.3	0.32±0.019	71.2±2.4	0.68±0.028	945±11.6	667.3±31.5
900	-0.52±0.033	0.35±0.03	-0.24±0.016	2.5±0.3	0.32±0.018	71.2±2.4	0.68±0.032	945±11.6	667.3±28.2
910	-0.52±0.037	0.35±0.03	-0.24±0.018	2.5±0.3	0.32±0.021	71.2±2.4	0.68±0.029	945±11.6	667.3±31.9

[a] The average lifetime of PL at a certain wavelength was calculated according to eqn.: $\bar{\tau} = \sum_{i=1}^{4} A_i \tau_i / \sum_{i=1}^{4} A_i (A_i > 0)$.

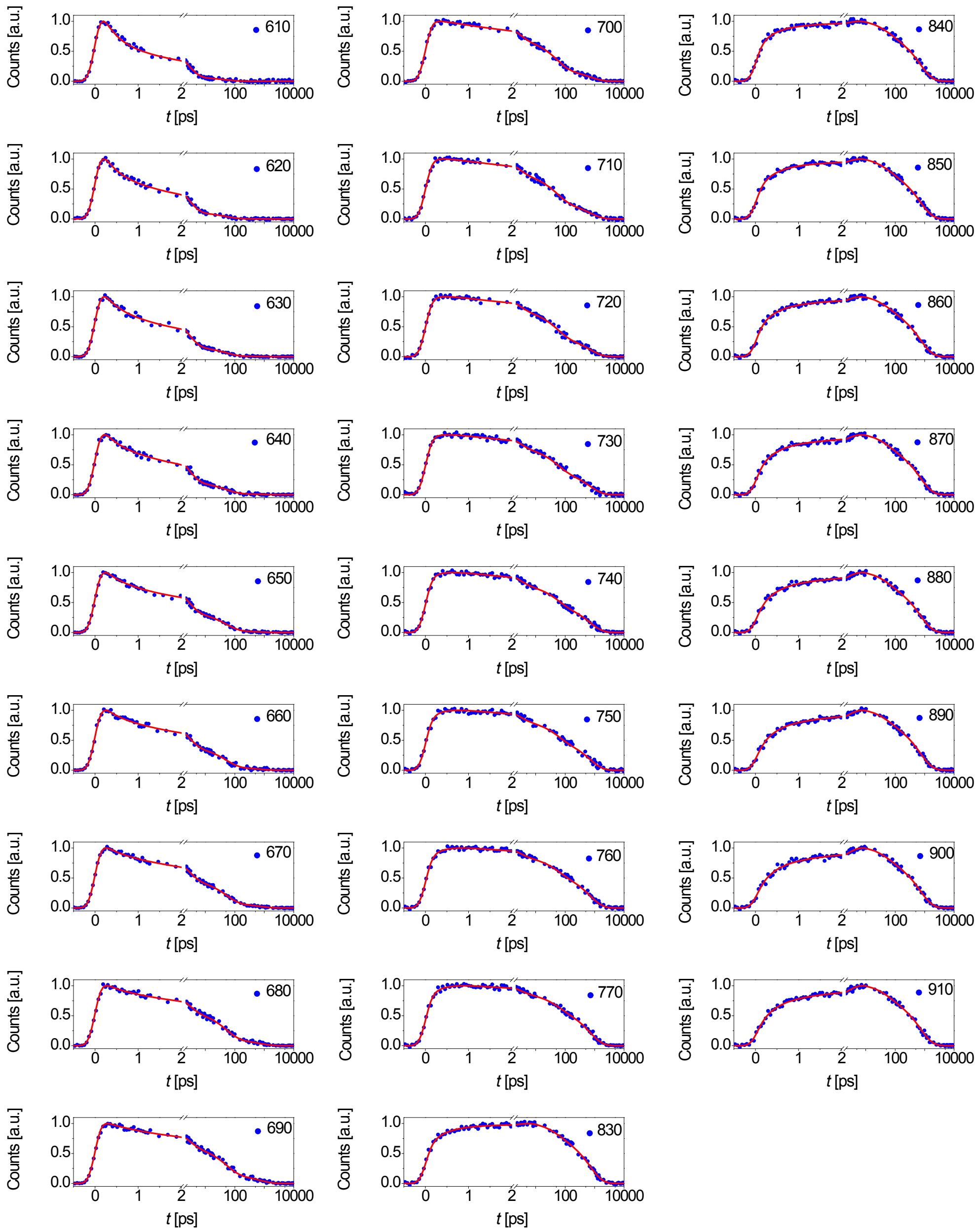

Fig. S12. PL traces (blue dots) of a **SC-3** grafted alumina film in contact with an electrolyte probed at a series of wavelengths. Note that PL intensities at different wavelengths have been normalized. The red solid lines are fittings via eqn.: $I_{PL} = I_0 + \sum_{i=1}^{4} A_i \exp(-t/\tau_i) \otimes \mathrm{IRF}$. Excitation wavelength: 490 nm.

Table S7. Time constants and amplitudes employed to fit PL traces for a **SC-3** grafted alumina film in contact with an electrolyte [a]

λ [nm]	A_1	τ_1 [ps]	A_2	τ_2 [ps]	A_3	τ_3 [ps]	A_4	τ_4 [ps]	$\bar{\tau}$ [ps]
610	0.52±0.032	0.33±0.03	0.44±0.032	2.3±0.1	0.04±0.003	51.4±1.2	0	693.1±9.7	3.3±0.2
620	0.43±0.033	0.33±0.03	0.50±0.032	2.3±0.1	0.07±0.005	51.4±1.2	0	693.1±9.7	6.1±0.3
630	0.35±0.029	0.33±0.03	0.53±0.036	2.3±0.1	0.11±0.008	51.4±1.2	0.01±0.001	693.1±9.7	11.3±1.1
640	0.31±0.027	0.33±0.03	0.54±0.029	2.3±0.1	0.14±0.010	51.4±1.2	0.01±0.001	693.1±9.7	18.6±1.2
650	0.25±0.020	0.33±0.03	0.49±0.031	2.3±0.1	0.24±0.021	51.4±1.2	0.02±0.001	693.1±9.7	28.5±1.8
660	0.20±0.016	0.33±0.03	0.48±0.033	2.3±0.1	0.28±0.017	51.4±1.2	0.04±0.002	693.1±9.7	42.1±2.3
670	0.15±0.012	0.33±0.03	0.46±0.028	2.3±0.1	0.33±0.020	51.4±1.2	0.06±0.003	693.1±9.7	61.8±3.2
680	0.11±0.008	0.33±0.03	0.40±0.027	2.3±0.1	0.40±0.025	51.4±1.2	0.09±0.005	693.1±9.7	85.3±4.8
690	0.06±0.004	0.33±0.03	0.39±0.025	2.3±0.1	0.42±0.027	51.4±1.2	0.13±0.010	693.1±9.7	114.8±8.4
700	-0.07±0.003	0.33±0.03	0.36±0.020	2.3±0.1	0.46±0.030	51.4±1.2	0.18±0.012	693.1±9.7	149.1±10.0
710	-0.14±0.012	0.33±0.03	0.32±0.023	2.3±0.1	0.43±0.032	51.4±1.2	0.25±0.017	693.1±9.7	195.3±13.6
720	-0.16±0.013	0.33±0.03	0.29±0.021	2.3±0.1	0.41±0.033	51.4±1.2	0.30±0.021	693.1±9.7	226.7±16.5
730	-0.19±0.014	0.33±0.03	0.28±0.019	2.3±0.1	0.36±0.028	51.4±1.2	0.36±0.024	693.1±9.7	265.1±18.3
740	-0.25±0.021	0.33±0.03	0.28±0.021	2.3±0.1	0.31±0.024	51.4±1.2	0.41±0.027	693.1±9.7	300.2±20.2
750	-0.32±0.022	0.33±0.03	0.25±0.020	2.3±0.1	0.30±0.021	51.4±1.2	0.45±0.030	693.1±9.7	325.1±22.2
760	-0.34±0.020	0.33±0.03	0.22±0.016	2.3±0.1	0.27±0.022	51.4±1.2	0.51±0.032	693.1±9.7	365.5±23.6
770	-0.35±0.021	0.33±0.03	0.21±0.014	2.3±0.1	0.24±0.019	51.4±1.2	0.55±0.032	693.1±9.7	397.6±23.5
830	-0.40±0.030	0.33±0.03	-0.12±0.008	2.3±0.1	0.24±0.017	51.4±1.2	0.76±0.033	693.1±9.7	537.0±24.1
840	-0.42±0.019	0.33±0.03	-0.16±0.011	2.3±0.1	0.24±0.017	51.4±1.2	0.76±0.036	693.1±9.7	537.0±26.2
850	-0.44±0.021	0.33±0.03	-0.21±0.013	2.3±0.1	0.24±0.016	51.4±1.2	0.76±0.035	693.1±9.7	537.0±25.4
860	-0.46±0.024	0.33±0.03	-0.24±0.014	2.3±0.1	0.24±0.020	51.4±1.2	0.76±0.032	693.1±9.7	537.0±23.5
870	-0.48±0.023	0.33±0.03	-0.27±0.017	2.3±0.1	0.24±0.021	51.4±1.2	0.76±0.029	693.1±9.7	537.0±20.5
880	-0.49±0.025	0.33±0.03	-0.31±0.019	2.3±0.1	0.24±0.018	51.4±1.2	0.76±0.034	693.1±9.7	537.0±24.8
890	-0.49±0.026	0.33±0.03	-0.34±0.020	2.3±0.1	0.24±0.016	51.4±1.2	0.76±0.035	693.1±9.7	537.0±25.4
900	-0.49±0.029	0.33±0.03	-0.36±0.022	2.3±0.1	0.24±0.012	51.4±1.2	0.76±0.031	693.1±9.7	537.0±22.4
910	-0.49±0.031	0.33±0.03	-0.36±0.024	2.3±0.1	0.24±0.016	51.4±1.2	0.76±0.036	693.1±9.7	537.0±26.1

[a] The average lifetime of PL at a certain wavelength was calculated according to eqn.: $\bar{\tau} = \sum_{i=1}^{4} A_i \tau_i \,/\, \sum_{i=1}^{4} A_i (A_i > 0)$.

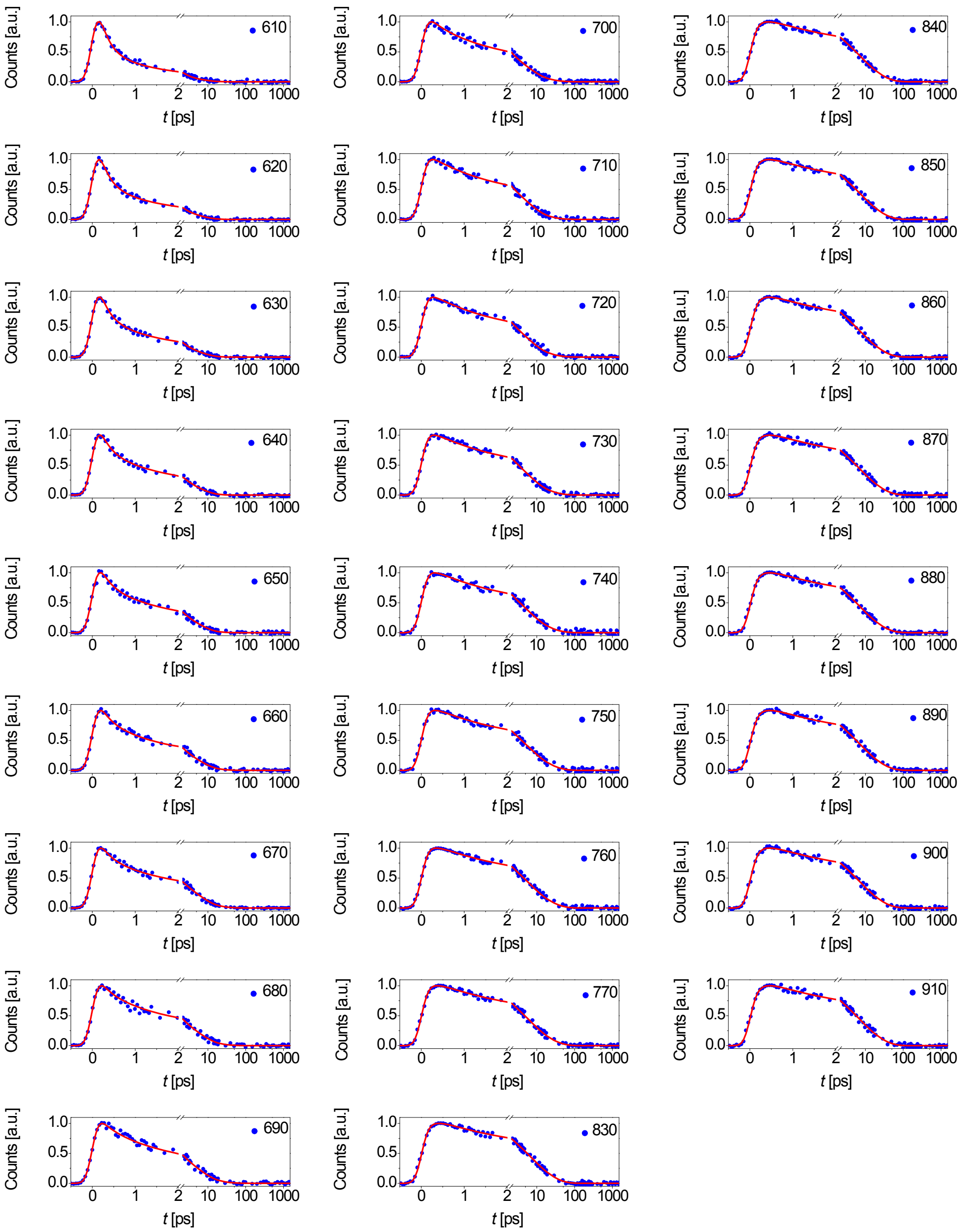

Fig. S14. PL traces (blue dots) of a **SC-1** grafted titania film in contact with an electrolyte probed at a series of wavelengths. Note that PL intensities at different wavelengths have been normalized. The red solid lines are fittings via eqn.: $I_{\mathrm{PL}} = I_0 + \sum_{i=1}^{4} A_i \exp(-t/\tau_i) \otimes \mathrm{IRF}$. Excitation wavelength: 490 nm.

Table S8. Time constants and amplitudes employed to fit PL traces for a **SC-1** grafted titania film in contact with an electrolyte [a]

λ [nm]	A_1	τ_1 [ps]	A_2	τ_2 [ps]	A_3	τ_3 [ps]	A_4	τ_4 [ps]	$\bar{\tau}$ [ps]
610	0.73±0.042	0.21±0.02	0.22±0.017	1.1±0.1	0.05±0.004	5.7±0.2	0	19.8±0.8	0.69±0.02
620	0.68±0.039	0.21±0.02	0.24±0.016	1.1±0.1	0.08±0.003	5.7±0.2	0	19.8±0.8	0.88±0.02
630	0.63±0.027	0.21±0.02	0.25±0.020	1.1±0.1	0.12±0.010	5.7±0.2	0	19.8±0.8	1.1±0.06
640	0.52±0.032	0.21±0.02	0.30±0.022	1.1±0.1	0.18±0.012	5.7±0.2	0	19.8±0.8	1.5±0.07
650	0.44±0.030	0.21±0.02	0.33±0.026	1.1±0.1	0.22±0.016	5.7±0.2	0.01±0.001	19.8±0.8	1.8±0.1
660	0.39±0.029	0.21±0.02	0.35±0.028	1.1±0.1	0.24±0.017	5.7±0.2	0.02±0.001	19.8±0.8	2.2±0.1
670	0.34±0.026	0.21±0.02	0.35±0.031	1.1±0.1	0.27±0.020	5.7±0.2	0.04±0.002	19.8±0.8	2.7±0.2
680	0.26±0.019	0.21±0.02	0.38±0.030	1.1±0.1	0.31±0.021	5.7±0.2	0.05±0.003	19.8±0.8	3.2±0.3
690	0.15±0.010	0.21±0.02	0.42±0.032	1.1±0.1	0.36±0.025	5.7±0.2	0.07±0.004	19.8±0.8	3.8±0.2
700	0.09±0.006	0.21±0.02	0.47±0.033	1.1±0.1	0.36±0.024	5.7±0.2	0.09±0.006	19.8±0.8	4.3±0.4
710	-0.10±0.004	0.21±0.02	0.45±0.034	1.1±0.1	0.45±0.023	5.7±0.2	0.10±0.007	19.8±0.8	5.1±0.3
720	-0.14±0.008	0.21±0.02	0.42±0.031	1.1±0.1	0.45±0.029	5.7±0.2	0.13±0.010	19.8±0.8	5.6±0.3
730	-0.19±0.012	0.21±0.02	0.37±0.029	1.1±0.1	0.46±0.030	5.7±0.2	0.17±0.012	19.8±0.8	6.3±0.4
740	-0.23±0.017	0.21±0.02	0.36±0.027	1.1±0.1	0.44±0.032	5.7±0.2	0.20±0.014	19.8±0.8	6.9±0.4
750	-0.26±0.016	0.21±0.02	0.34±0.028	1.1±0.1	0.41±0.027	5.7±0.2	0.25±0.017	19.8±0.8	7.6±0.5
760	-0.31±0.020	0.21±0.02	0.30±0.025	1.1±0.1	0.42±0.026	5.7±0.2	0.28±0.021	19.8±0.8	8.3±0.5
770	-0.36±0.022	0.21±0.02	0.29±0.022	1.1±0.1	0.41±0.027	5.7±0.2	0.30±0.024	19.8±0.8	8.6±0.6
830	-0.41±0.028	0.21±0.02	0.26±0.021	1.1±0.1	0.38±0.021	5.7±0.2	0.36±0.021	19.8±0.8	9.6±0.6
840	-0.43±0.030	0.21±0.02	0.26±0.020	1.1±0.1	0.38±0.019	5.7±0.2	0.36±0.019	19.8±0.8	9.6±0.5
850	-0.45±0.032	0.21±0.02	0.26±0.021	1.1±0.1	0.38±0.019	5.7±0.2	0.36±0.021	19.8±0.8	9.6±0.5
860	-0.48±0.031	0.21±0.02	0.26±0.020	1.1±0.1	0.38±0.023	5.7±0.2	0.36±0.023	19.8±0.8	9.6±0.6
870	-0.49±0.033	0.21±0.02	0.26±0.023	1.1±0.1	0.38±0.022	5.7±0.2	0.36±0.020	19.8±0.8	9.6±0.7
880	-0.50±0.038	0.21±0.02	0.26±0.022	1.1±0.1	0.38±0.023	5.7±0.2	0.36±0.017	19.8±0.8	9.6±0.7
890	-0.51±0.036	0.21±0.02	0.26±0.017	1.1±0.1	0.38±0.025	5.7±0.2	0.36±0.019	19.8±0.8	9.6±0.6
900	-0.51±0.029	0.21±0.02	0.26±0.016	1.1±0.1	0.38±0.017	5.7±0.2	0.36±0.021	19.8±0.8	9.6±0.8
910	-0.51±0.030	0.21±0.02	0.26±0.018	1.1±0.1	0.38±0.021	5.7±0.2	0.36±0.016	19.8±0.8	9.6±0.6

[a] The average lifetime of PL at a certain wavelength was calculated according to eqn.: $\bar{\tau} = \sum_{i=1}^{4} A_i \tau_i \,/\, \sum_{i=1}^{4} A_i (A_i > 0)$.

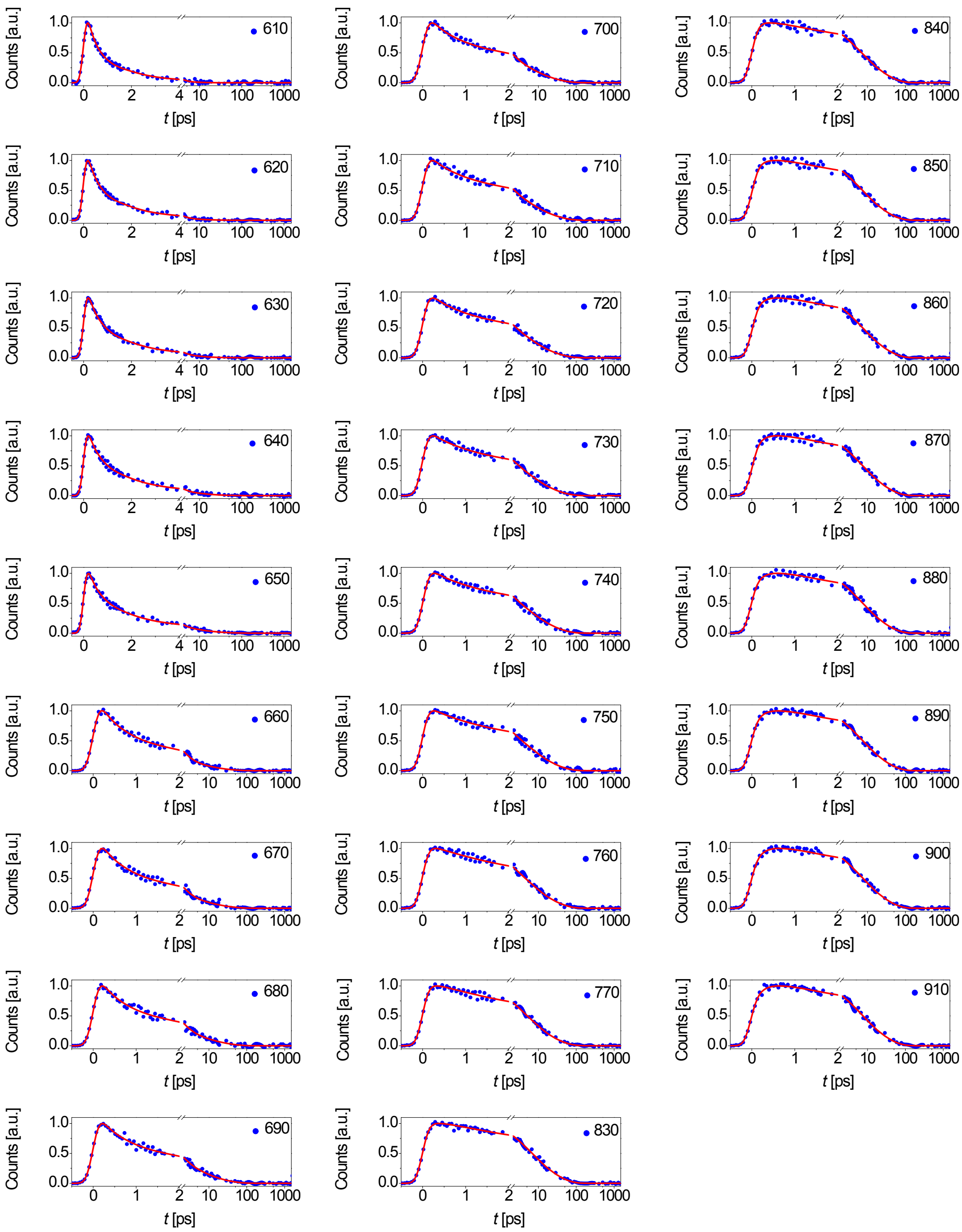

Fig. S14. PL traces (blue dots) of a **SC-2** grafted titania film in contact with an electrolyte probed at a series of wavelengths. Note that PL intensities at different wavelengths have been normalized. The red solid lines are fittings via eqn.: $I_{\mathrm{PL}} = I_0 + \sum_{i=1}^{4} A_i \exp(-t/\tau_i) \otimes \mathrm{IRF}$. Excitation wavelength: 490 nm.

Table S9. Time constants and amplitudes employed to fit PL traces for a **SC-2** grafted titania film in contact with an electrolyte [a]

λ [nm]	A_1	τ_1 [ps]	A_2	τ_2 [ps]	A_3	τ_3 [ps]	A_4	τ_4 [ps]	$\bar{\tau}$ [ps]
610	0.58±0.034	0.28±0.03	0.40±0.028	1.4±0.1	0.02±0.001	6.6±0.4	0	28.1±1.1	0.82±0.01
620	0.51±0.028	0.28±0.03	0.45±0.029	1.4±0.1	0.03±0.002	6.6±0.4	0.01±0.001	28.1±1.1	1.1±0.04
630	0.45±0.035	0.28±0.03	0.49±0.033	1.4±0.1	0.05±0.003	6.6±0.4	0.01±0.001	28.1±1.1	1.4±0.05
640	0.40±0.027	0.28±0.03	0.52±0.035	1.4±0.1	0.06±0.004	6.6±0.4	0.02±0.001	28.1±1.1	1.7±0.06
650	0.39±0.025	0.28±0.03	0.51±0.037	1.4±0.1	0.07±0.005	6.6±0.4	0.03±0.002	28.1±1.1	2.2±0.09
660	0.35±0.021	0.28±0.03	0.51±0.028	1.4±0.1	0.09±0.007	6.6±0.4	0.05±0.003	28.1±1.1	2.7±0.1
670	0.33±0.020	0.28±0.03	0.51±0.029	1.4±0.1	0.10±0.004	6.6±0.4	0.06±0.003	28.1±1.1	3.2±0.1
680	0.31±0.021	0.28±0.03	0.49±0.032	1.4±0.1	0.12±0.008	6.6±0.4	0.08±0.004	28.1±1.1	3.8±0.2
690	0.26±0.019	0.28±0.03	0.46±0.032	1.4±0.1	0.18±0.011	6.6±0.4	0.10±0.006	28.1±1.1	4.6±0.3
700	0.24±0.016	0.28±0.03	0.43±0.021	1.4±0.1	0.20±0.013	6.6±0.4	0.13±0.010	28.1±1.1	5.5±0.4
710	0.19±0.013	0.28±0.03	0.41±0.029	1.4±0.1	0.25±0.017	6.6±0.4	0.15±0.011	28.1±1.1	6.6±0.4
720	0.16±0.012	0.28±0.03	0.39±0.030	1.4±0.1	0.28±0.019	6.6±0.4	0.17±0.012	28.1±1.1	7.3±0.5
730	0.11±0.009	0.28±0.03	0.38±0.031	1.4±0.1	0.31±0.021	6.6±0.4	0.20±0.013	28.1±1.1	8.3±0.6
740	0.07±0.005	0.28±0.03	0.38±0.030	1.4±0.1	0.33±0.023	6.6±0.4	0.22±0.015	28.1±1.1	9.0±0.6
750	0.03±0.002	0.28±0.03	0.37±0.031	1.4±0.1	0.36±0.025	6.6±0.4	0.24±0.016	28.1±1.1	9.8±0.7
760	-0.11±0.006	0.28±0.03	0.34±0.028	1.4±0.1	0.40±0.024	6.6±0.4	0.26±0.017	28.1±1.1	10.4±0.8
770	-0.17±0.012	0.28±0.03	0.31±0.027	1.4±0.1	0.42±0.030	6.6±0.4	0.27±0.021	28.1±1.1	10.9±0.9
830	-0.20±0.015	0.28±0.03	0.19±0.015	1.4±0.1	0.45±0.031	6.6±0.4	0.36±0.026	28.1±1.1	13.3±0.9
840	-0.24±0.018	0.28±0.03	0.19±0.013	1.4±0.1	0.45±0.032	6.6±0.4	0.36±0.024	28.1±1.1	13.3±0.8
850	-0.30±0.023	0.28±0.03	0.19±0.012	1.4±0.1	0.45±0.030	6.6±0.4	0.36±0.022	28.1±1.1	13.3±1.0
860	-0.39±0.023	0.28±0.03	0.19±0.017	1.4±0.1	0.45±0.029	6.6±0.4	0.36±0.026	28.1±1.1	13.3±1.1
870	-0.44±0.026	0.28±0.03	0.19±0.015	1.4±0.1	0.45±0.032	6.6±0.4	0.36±0.025	28.1±1.1	13.3±1.0
880	-0.48±0.031	0.28±0.03	0.19±0.014	1.4±0.1	0.45±0.031	6.6±0.4	0.36±0.027	28.1±1.1	13.3±0.9
890	-0.50±0.021	0.28±0.03	0.19±0.015	1.4±0.1	0.45±0.028	6.6±0.4	0.36±0.030	28.1±1.1	13.3±1.0
900	-0.54±0.033	0.28±0.03	0.19±0.016	1.4±0.1	0.45±0.027	6.6±0.4	0.36±0.031	28.1±1.1	13.3±1.1
910	-0.54±0.034	0.28±0.03	0.19±0.017	1.4±0.1	0.45±0.029	6.6±0.4	0.36±0.032	28.1±1.1	13.3±1.1

[a] The average lifetime of PL at a certain wavelength was calculated according to eqn.: $\bar{\tau} = \sum_{i=1}^{4} A_i \tau_i / \sum_{i=1}^{4} A_i (A_i > 0)$.

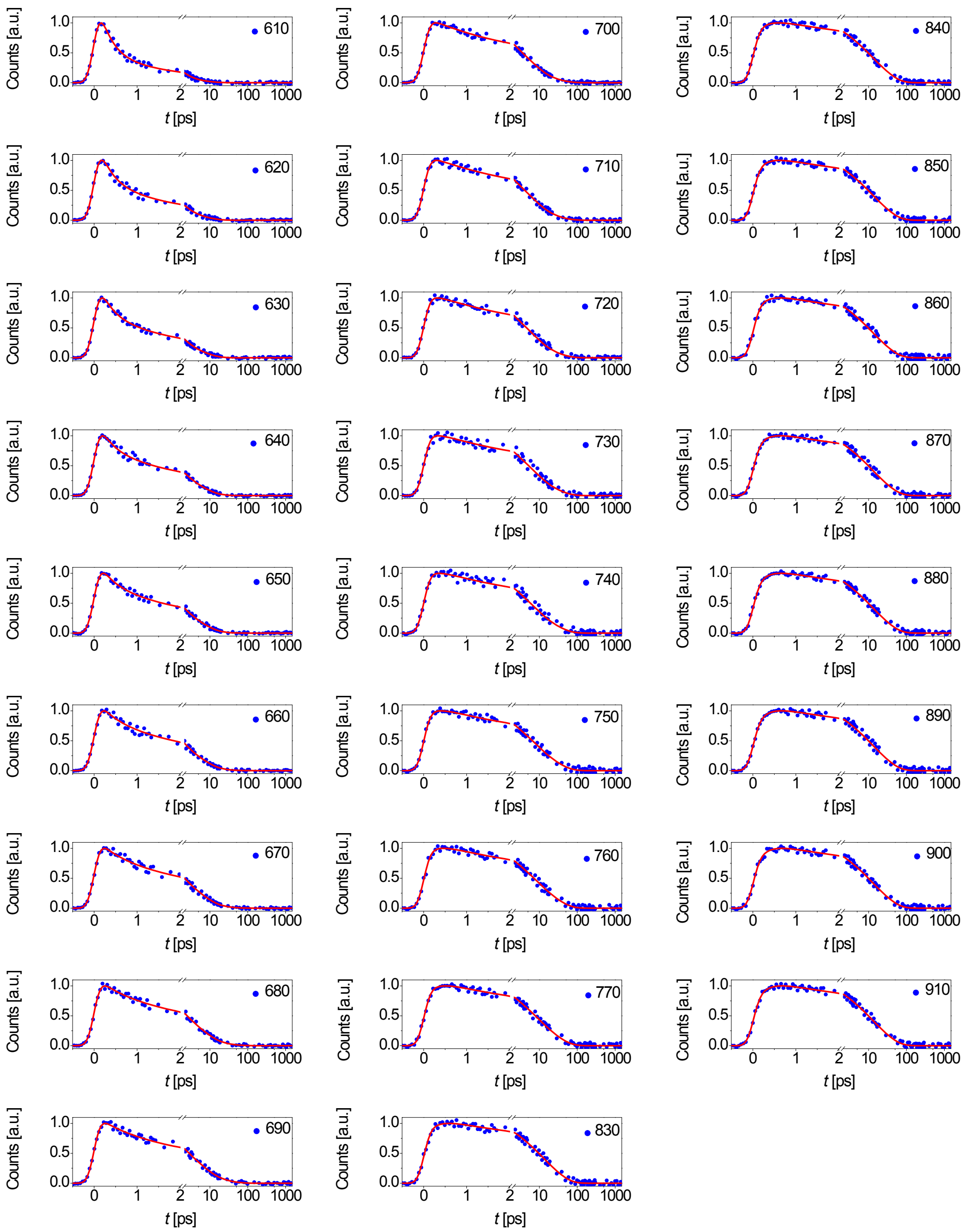

Fig. S15. PL traces (blue dots) of a **SC-3** grafted titania film in contact with an electrolyte probed at a series of wavelengths. Note that PL intensities at different wavelengths have been normalized. The red solid lines are fittings via eqn.: $I_{PL} = I_0 + \sum_{i=1}^{4} A_i \exp(-t/\tau_i) \otimes \mathrm{IRF}$. Excitation wavelength: 490 nm.

Table S10. Time constants and amplitudes employed to fit PL traces for a **SC-3** grafted titania film in contact with an electrolyte [a]

λ [nm]	A_1	τ_1 [ps]	A_2	τ_2 [ps]	A_3	τ_3 [ps]	A_4	τ_4 [ps]	$\bar{\tau}$ [ps]
610	0.69±0.035	0.27±0.02	0.26±0.021	1.3±0.1	0.05±0.004	6.4±0.3	0	25.9±1.2	0.85±0.03
620	0.54±0.042	0.27±0.02	0.35±0.022	1.3±0.1	0.11±0.005	6.4±0.3	0	25.9±1.2	1.3±0.03
630	0.47±0.031	0.27±0.02	0.36±0.027	1.3±0.1	0.17±0.012	6.4±0.3	0	25.9±1.2	1.7±0.08
640	0.38±0.028	0.27±0.02	0.36±0.025	1.3±0.1	0.25±0.020	6.4±0.3	0.01±0.001	25.9±1.2	2.3±0.2
650	0.29±0.024	0.27±0.02	0.40±0.021	1.3±0.1	0.29±0.022	6.4±0.3	0.02±0.001	25.9±1.2	2.8±0.2
660	0.19±0.016	0.27±0.02	0.45±0.032	1.3±0.1	0.33±0.027	6.4±0.3	0.03±0.002	25.9±1.2	3.5±0.3
670	0.12±0.010	0.27±0.02	0.45±0.030	1.3±0.1	0.38±0.025	6.4±0.3	0.05±0.003	25.9±1.2	4.4±0.2
680	0.07±0.005	0.27±0.02	0.43±0.031	1.3±0.1	0.42±0.023	6.4±0.3	0.08±0.005	25.9±1.2	5.4±0.3
690	0.05±0.004	0.27±0.02	0.40±0.027	1.3±0.1	0.44±0.023	6.4±0.3	0.11±0.007	25.9±1.2	6.3±0.4
700	-0.07±0.005	0.27±0.02	0.36±0.026	1.3±0.1	0.48±0.030	6.4±0.3	0.16±0.013	25.9±1.2	7.6±0.6
710	-0.10±0.007	0.27±0.02	0.31±0.020	1.3±0.1	0.50±0.034	6.4±0.3	0.19±0.013	25.9±1.2	8.5±0.6
720	-0.15±0.011	0.27±0.02	0.29±0.021	1.3±0.1	0.49±0.032	6.4±0.3	0.22±0.015	25.9±1.2	9.3±0.7
730	-0.18±0.012	0.27±0.02	0.27±0.022	1.3±0.1	0.45±0.030	6.4±0.3	0.28±0.017	25.9±1.2	10.4±0.8
740	-0.21±0.016	0.27±0.02	0.27±0.020	1.3±0.1	0.41±0.031	6.4±0.3	0.32±0.021	25.9±1.2	11.4±0.8
750	-0.26±0.020	0.27±0.02	0.26±0.021	1.3±0.1	0.37±0.028	6.4±0.3	0.37±0.024	25.9±1.2	12.3±0.9
760	-0.31±0.026	0.27±0.02	0.24±0.018	1.3±0.1	0.36±0.024	6.4±0.3	0.40±0.027	25.9±1.2	13.1±1.0
770	-0.36±0.021	0.27±0.02	0.22±0.016	1.3±0.1	0.35±0.020	6.4±0.3	0.43±0.030	25.9±1.2	13.7±1.0
830	-0.39±0.023	0.27±0.02	0.17±0.012	1.3±0.1	0.30±0.019	6.4±0.3	0.53±0.031	25.9±1.2	15.8±1.0
840	-0.41±0.026	0.27±0.02	0.17±0.013	1.3±0.1	0.30±0.021	6.4±0.3	0.53±0.032	25.9±1.2	15.8±1.1
850	-0.43±0.027	0.27±0.02	0.17±0.012	1.3±0.1	0.30±0.022	6.4±0.3	0.53±0.033	25.9±1.2	15.8±1.2
860	-0.44±0.030	0.27±0.02	0.17±0.011	1.3±0.1	0.30±0.024	6.4±0.3	0.53±0.035	25.9±1.2	15.8±1.2
870	-0.46±0.032	0.27±0.02	0.17±0.015	1.3±0.1	0.30±0.022	6.4±0.3	0.53±0.038	25.9±1.2	15.8±1.1
880	-0.49±0.031	0.27±0.02	0.17±0.012	1.3±0.1	0.30±0.021	6.4±0.3	0.53±0.040	25.9±1.2	15.8±1.1
890	-0.51±10.035	0.27±0.02	0.17±0.013	1.3±0.1	0.30±0.019	6.4±0.3	0.53±0.037	25.9±1.2	15.8±1.1
900	-0.52±0.036	0.27±0.02	0.17±0.014	1.3±0.1	0.30±0.022	6.4±0.3	0.53±0.035	25.9±1.2	15.8±1.0
910	-0.52±0.032	0.27±0.02	0.17±0.015	1.3±0.1	0.30±0.019	6.4±0.3	0.53±0.032	25.9±1.2	15.8±1.0

[a] The average lifetime of PL at a certain wavelength was calculated according to eqn.: $\bar{\tau} = \sum_{i=1}^{4} A_i \tau_i / \sum_{i=1}^{4} A_i (A_i > 0)$.

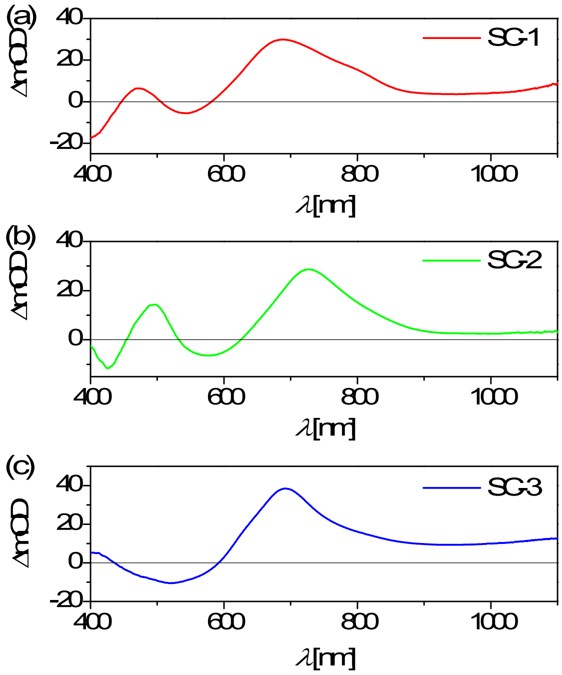

Fig. S16. Wavelength-dependent absorption change upon applying a positive potential bias to a 1.2-μm-thick, dye-grafted titania film immersed in EMITFSI.